NAVAL POSTGRADUATE SCHOOL
Monterey, California

THESIS

ANALYSIS OF LARGE AREA SYNCHRONOUS CODE-DIVISION MULTIPLE ACCESS (LAS-CDMA)

by

Stephen A. Brooks

June 2002

Thesis Advisor:	R. Clark Robertson
Co-Advisor:	Tri T. Ha

THIS PAGE INTENTIONALLY LEFT BLANK

REPORT DOCUMENTATION PAGE			Form Approved OMB No. 0704-0188
Public reporting burden for this collection of information is estimated to average 1 hour per response, including the time for reviewing instruction, searching existing data sources, gathering and maintaining the data needed, and completing and reviewing the collection of information. Send comments regarding this burden estimate or any other aspect of this collection of information, including suggestions for reducing this burden, to Washington headquarters Services, Directorate for Information Operations and Reports, 1215 Jefferson Davis Highway, Suite 1204, Arlington, VA 22202-4302, and to the Office of Management and Budget, Paperwork Reduction Project (0704-0188) Washington DC 20503.			
1. AGENCY USE ONLY *(Leave blank)*	**2. REPORT DATE** June 2002	**3. REPORT TYPE AND DATES COVERED** Master's Thesis	
4. TITLE AND SUBTITLE: Title (Mix case letters) Analysis of Large Area Synchronous Code-Division Multiple Access (LAS-CDMA)			**5. FUNDING NUMBERS**
6. AUTHOR(S) Brooks, Stephen A.			
7. PERFORMING ORGANIZATION NAME(S) AND ADDRESS(ES) Naval Postgraduate School Monterey, CA 93943-5000			**8. PERFORMING ORGANIZATION REPORT NUMBER**
9. SPONSORING /MONITORING AGENCY NAME(S) AND ADDRESS(ES) N/A			**10. SPONSORING/MONITORING AGENCY REPORT NUMBER**
11. SUPPLEMENTARY NOTES The views expressed in this thesis are those of the author and do not reflect the official policy or position of the Department of Defense or the U.S. Government.			
12a. DISTRIBUTION / AVAILABILITY STATEMENT Approved for public release; distribution is unlimited.			**12b. DISTRIBUTION CODE**

13. ABSTRACT ***(maximum 200 words)***

Large area synchronous code-division multiple access (LAS-CDMA) is a proposed fourth generation cellular standard. Similar to cdma2000, the distinguishing feature of LAS-CDMA is the new set of spreading codes used to separate users in the wireless channel. This thesis examines the properties of the new spreading codes. Unlike Walsh functions, which are orthogonal only when perfectly synchronized, LAS-CDMA spreading codes are orthogonal when synchronized within a nine-chip interference-free time window. The interference-free time window allows LAS-CDMA to transmit the forward link and reverse link over the same frequency band. The primary LAS-CDMA data channels are examined. LAS-CDMA uses a separate set of modulation and coding rate combinations for voice and data communications. Analysis of the effect of a tone jammer on the modulation and coding rate combinations is presented. Also, the ease with which LAS-CDMA can be intercepted is examined, and the security of LAS-CDMA is analyzed.

14. SUBJECT TERMS Cellular Communications, CDMA, Tone Jammer, Synchronization			**15. NUMBER OF PAGES** 105
			16. PRICE CODE
17. SECURITY CLASSIFICATION OF REPORT Unclassified	**18. SECURITY CLASSIFICATION OF THIS PAGE** Unclassified	**19. SECURITY CLASSIFICATION OF ABSTRACT** Unclassified	**20. LIMITATION OF ABSTRACT** UL

NSN 7540-01-280-5500 Standard Form 298 (Rev. 2-89)
Prescribed by ANSI Std. 239-18

THIS PAGE INTENTIONALLY LEFT BLANK

Approved for public release; distribution is unlimited.

ANALYSIS OF LARGE AREA SYNCHRONOUS CODE-DIVISION MULTIPLE ACCESS (LAS-CDMA)

Stephen A. Brooks
Ensign, United States Navy
B.S., United States Naval Academy, 2001

Submitted in partial fulfillment of the
requirements for the degree of

MASTER OF SCIENCE IN ELECTRICAL ENGINEERING

from the

NAVAL POSTGRADUATE SCHOOL
June 2002

Author: Stephen A. Brooks

Approved by: R. Clark Robertson
Thesis Advisor

Tri T. Ha
Co-Advisor

Jeffery B. Knorr
Chairman, Department of Electrical and Computer Engineering

THIS PAGE INTENTIONALLY LEFT BLANK

ABSTRACT

Large area synchronous code-division multiple access (LAS-CDMA) is a proposed fourth generation cellular standard. Similar to cdma2000, the distinguishing feature of LAS-CDMA is the new set of spreading codes used to separate users in the wireless channel. This thesis examines the properties of the new spreading codes. Unlike Walsh functions, which are orthogonal only when perfectly synchronized, LAS-CDMA spreading codes are orthogonal when synchronized within a nine-chip interference-free time window. The interference-free time window allows LAS-CDMA to transmit the forward link and reverse link over the same frequency band. The primary LAS-CDMA data channels are examined in this thesis. LAS-CDMA uses a separate set of modulation and coding rate combinations for voice and data communications. Analysis of the effect of a tone jammer on the modulation and coding rate combinations is presented. Also, the ease with which LAS-CDMA can be intercepted is examined, and the security of LAS-CDMA is analyzed.

THIS PAGE INTENTIONALLY LEFT BLANK

TABLE OF CONTENTS

LIST OF FIGURES

LIST OF TABLES

THIS PAGE INTENTIONALLY LEFT BLANK

EXECUTIVE SUMMARY

Cellular technology has improved since U.S. Advanced Mobile Phone System (AMPS) became the first commercial cellular system available in the United States in 1983. Code-division multiple access (CDMA) systems allow multiple users to communicate over the same frequency band by using orthogonal codes to separate users. Proposed third generation CDMA systems use Walsh functions to separate users. Walsh functions are only orthogonal when perfectly synchronized. Cellular communications are broadcast through a wireless channel that introduces a multipath delay spread. The spread reduces the ability of the Walsh functions to eliminate interference from other users of the wireless channel.

Unlike Walsh functions, the LAS spreading codes used by large area synchronous CDMA (LAS-CDMA) are orthogonal over a nine-chip interference-free window. The LAS spreading codes are formed by separating LS code intervals with gaps determined by the LA code. The LS codes separate users within a coverage area, while the LA codes are used to separate coverage areas. The interference-free window allows LAS-CDMA to separate users in the wireless channel more effectively than systems that use Walsh functions to separate users. The interference-free window also enables LAS-CDMA to transmit the reverse link synchronously. Other CDMA systems must asynchronously transmit the reverse link because the systems are unable to synchronize the mobile stations within the coverage area closely enough to synchronously transmit the reverse link using Walsh functions. Using a synchronous reverse link, LAS-CDMA is able to transmit the reverse link at a higher data rate for a given signal-to-noise ratio than systems using an asynchronous reverse link.

LAS-CDMA transmits voice communications using different coding and modulation schemes than data communications. Voice communications are broadcasted on the Fundamental Channel using 16-QAM modulation and rate 2/3 convolutional coding. A constant symbol rate is maintained by repeating symbols according to the data rate. Data communications are broadcasted on the Packet Data Channel. The Packet

Data channel is modulated using QPSK, 8PSK, 16-QAM, or 64-QAM and is encoded using rate 1/2 or rate 3/4 convolutional coding. The assignment of more than one code channel to a single user increases the data rate on the Forward Packet Data Channel. The Fundamental Channel and Packet Data Channel are transmitted using modulation techniques that require coherent detection. Coherent detection requires that a pilot tone be transmitted. LAS-CDMA uses a burst pilot to minimize the loss of throughput due to the pilot tone.

Included in the discussion of the LAS-CDMA channels is the Forward Synchronization (Sync) Channel. The Forward Sync Channel informs mobile stations which LA code is used within the coverage area and the LS codes assigned to other channels. The Forward Sync Channel is easy to receive because the number of possible spreading codes has been restricted to 32, and the first chip of the Forward Sync Channel is delayed by an integer multiple of 20 ms frames from the GPS time reference. Unlike IS-95 or cdma2000, LAS-CDMA traffic channels are not masked by a long PN sequence that makes intercepting the channels more difficult. Before LAS-CDMA can be implemented as a commercial cellular standard, the security of information transmitted by LAS-CDMA needs to be improved.

One figure of merit for LAS-CDMA is the probability of correctly communicating through the wireless channel in the presence of additive white Gaussian noise and a tone jammer. The tone jammer is easy to implement because it does not require information about the coding or modulation of the jammed signal. The effect of the tone jammer is analyzed for all the modulation and coding combinations used by LAS-CDMA. The parameters of the Fundamental Channel configurations analyzed are listed in Table 1. The parameters of the Packet Data Channel configurations analyzed are listed Table 2. The results of the analysis on the effect of a tone jammer on the Fundamental Channel are displayed in Figure 1. The results of the analysis of the effect of a tone jammer on the Packet Data Channel are displayed in Figure 2.

Table 1. Fundamental Channel Parameters. After Ref [9].

Index	Code Rate	Modulation Type	LS Code Length	Symbol Repetition
FC1	2/3	16 QAM	128	1x
FC2	2/3	16 QAM	128	2x
FC3	2/3	16 QAM	128	4x
FC4	2/3	16 QAM	128	8x

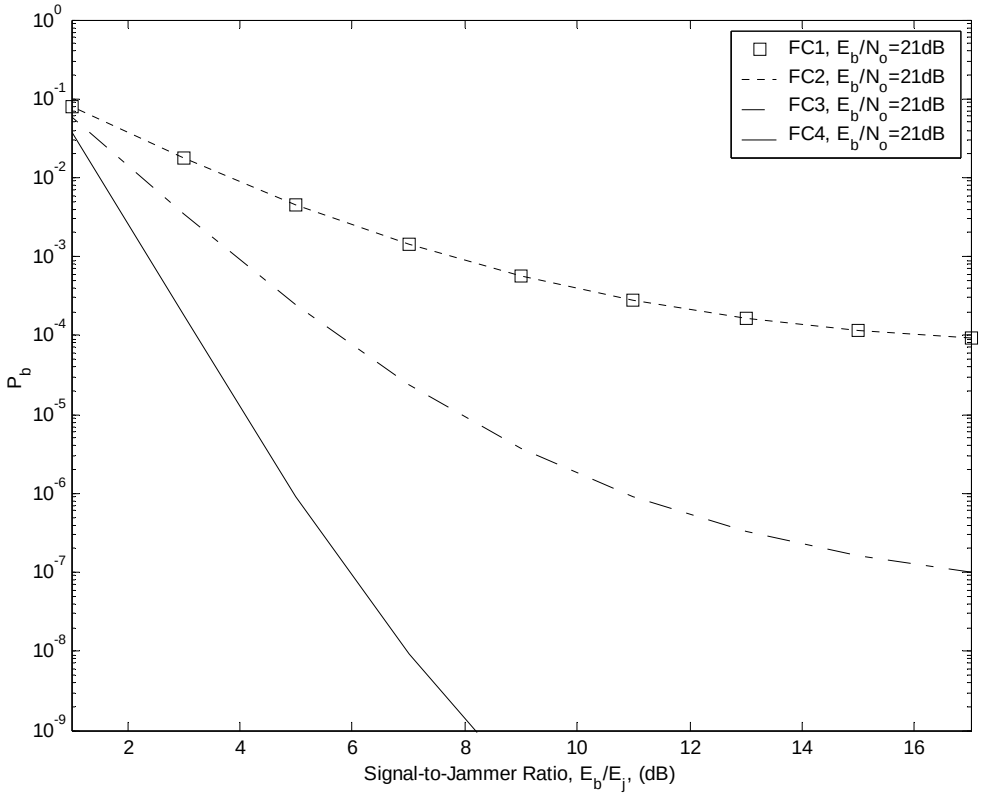

Figure 1. Bit Error Ratio Comparison for the Symbol Repetition Schemes used by the Fundamental Channel. The Signal-to-Noise Ratio is 21 dB.

Table 2. Packet Data Channel Parameters. After Ref [9].

MCS Index	Data Rate (kbps)	Code Rate	Modulation Type	LS Code Length
8	216xN	3/4	64QAM	16
7	144xN	1/2	64QAM	16
6	144xN	3/4	16QAM	16
5	96xN	1/2	16QAM	16
4	108xN	3/4	8PSK	16
3	72xN	1/2	8PSK	16
2	60xN	3/4	QPSK	16
1	40xN	1/2	QPSK	16

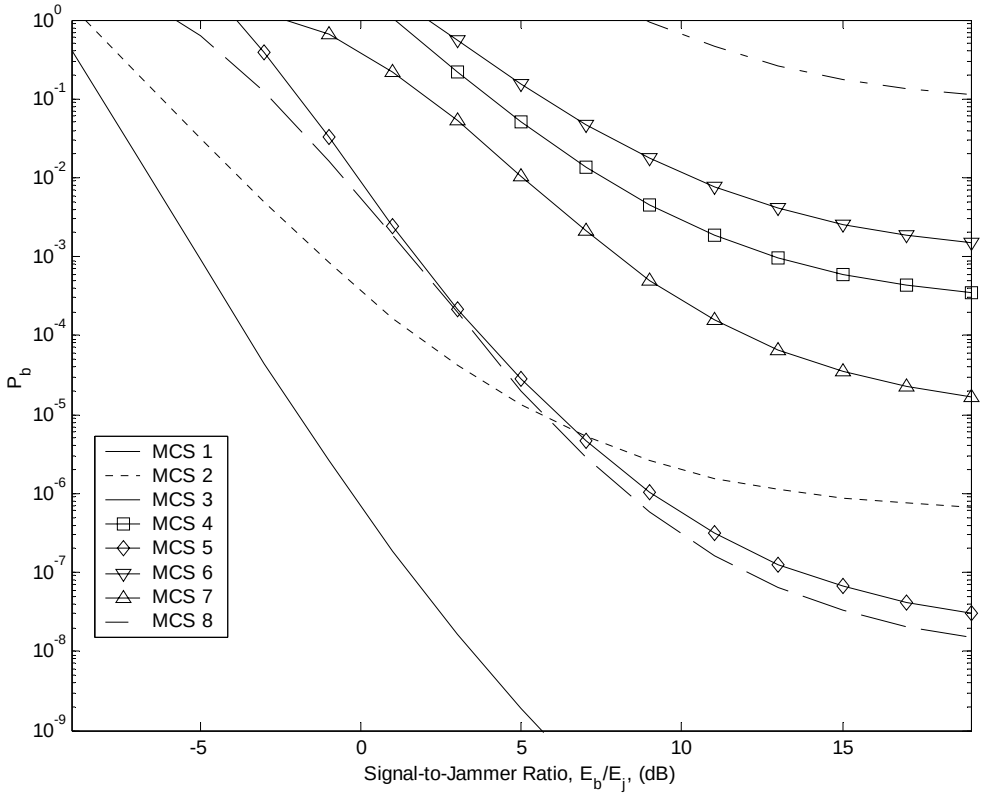

Figure 2. Bit Error Ratio Comparison for Modulation and Coding Schemes used by the Fundamental Channel. The Signal-to-Noise Ratio is 21 dB.

The results displayed in Figure 1 and Figure 2 indicate that a signal-to-jammer ratio of 0 dB will significantly reduce the performance of LAS-CDMA. A signal-to-jammer ratio of 0 dB would force LAS-CDMA to transmit the Packet Data Channel using QPSK and rate 1/2 convolutional coding to maintain a bit error ratio of 10^{-3} with a signal-to-noise ration of 21 dB.

The analysis results also illustrate the difference between the performance obtained with the rate 1/2 convolutional code and the rate 3/4 convolutional code in a Rayleigh fading channel. For the different modulation and coding schemes used by LAS-CDMA, we expect the performance to degrade as the data rate increases for a given signal-to-noise ratio. From the analysis, we conclude that the performance advantage of the rate 1/2 convolutional code in a Rayleigh fading channel is greater than the performance loss incurred by using higher order modulation schemes. Higher data rates and better performance are provided by higher order modulation and rate 1/2 convolutional coding than lower order modulation and rate 3/4 convolutional coding.

This thesis illustrates the need to reconsider the modulation and code rate pairs used by the Packet Data Channel. Specifically, the rate 3/4 convolutional code should be replaced so that the data rate of the modulation and code rate pairs decrease as performance in additive white Gaussian noise improves.

THIS PAGE INTENTIONALLY LEFT BLANK

I. INTRODUCTION

A. BACKGROUND

In the summer of 2000 Link Air completed the first call using large area-synchronous code-division multiple access (LAS-CDMA) technology and entered the competition to define the fourth generation cellular standard [1]. Link Air has deployed a trial LAS-CDMA network in Shanghai and demonstrated the system's capabilities by simultaneously transmitting voice and steaming video at 384 kbps to a moving vehicle [2]. LAS-CDMA is LinkAir's solution to challenges facing the third generation (3G) of cellular technology: a continued increase in the number of users, increased use as a substitute for traditional wired services, the integration of voice and data, and accommodation of asymmetric needs of the wireless internet. LAS-CDMA improves 3G services by utilizing a new set of spreading codes.

LAS-CDMA and 3G technologies will provide the ability for a mobile user to access more information than ever before. The ability for the mobile user to rapidly access and share data leads to increased security concerns. Cellular phones raise concerns about ability to protect information transmitted on the wireless channel and the ability to deny potential adversaries the capabilities provided by cellular systems. China has already taken measures to protect military information from being intercepted. Acknowledging the security risks for cellular phone communication, the People's Liberation Army of China has barred soldiers from using cellular phones and pagers [3]. This thesis will provide a background on LAS-CDMA and discuss ways to exploit LAS-CDMA.

B. OBJECTIVE

The objective of this thesis is to develop a strategy for exploiting LAS-CDMA and assess how secure LAS-CDMA transmissions are. Knowledge of the physical layer leads to strategies to detect, intercept, and jam LAS-CDMA. Methods of synchronizing and intercepting LAS-CDMA will be explored. This thesis will also examine the effect of a tone jammer on the modulation techniques utilized in LAS-CDMA. The effects of the

jammer will be presented as bit error ratios as a function of the signal-to-jamming noise ratio for a range of signal-to-noise ratios.

C. RELATED WORK

Although this thesis was not inspired directly by prior research, there have been a number of studies of related topics. The related work can be divided into two groups, research on the effect of jammers on digital communications and research on the exploitation of wireless communication systems.

The most relevant research on the security of wireless communication systems addresses security issues of wireless mobile communications in the context of tactical battlefield [4]. Security weaknesses of CDMA are identified and improvements are suggested. In addition, the effect of a pulse noise jammer on an IS-95 based system is presented.

Other research focuses on the effect of jammers on digital communications [5]. Simulation results display the effects of several varieties of jammers on coherently detected BFSK, BPSK, QPSK and noncoherently detected BFSK in the presence of additive white Gaussian noise (AWGN).

D. ORGANIZATION OF THESIS

An overview of LAS-CDMA will be provided in Chapter II. Emphasis will be placed on the spreading codes employed by LAS-CDMA, the techniques used to transmit voice data, and the techniques used to transmit high-speed data. Chapter III will examine methods of synchronizing with and intercepting LAS-CDMA. Analysis of the effect of a tone jammer on LAS-CDMA will be presented in Chapter IV. Conclusions and recommendations for further research are included in Chapter V.

II. LARGE AREA SYNCHRONOUS CODE DIVISION MULTIPLE ACCESS

A. DEVELOPMENT OF CELLULAR SYSTEMS

Since Doug Ring developed the cellular concept at Bell Laboratories in 1957 there has been a desire to increase the quantity and improve the quality of signals transmitted on radio frequencies [6]. These desires are evident in the development of cellular telephone technology. The first commercial cellular system available in the United States, U.S. Advanced Mobile Phone System (AMPS), is an analog system that uses frequency division to separate cellular channels. AMPS is limited because frequency division is not an efficient method of separating cellular channels and, being analog, AMPS could not take advantage of methods of error correction. AMPS has been replaced by digital cellular systems that separate cellular channels more efficiently. Two different methods of separating cellular channels have been developed to increase the capacity of cellular systems. Time-division multiple access (TDMA) divides the frequency channels used to transmit and receive into time slots. In each slot only one user is allowed to transmit or receive. Although TDMA supports more users than frequency division, it is less efficient than code-division multiple access (CDMA)

All cellular systems reuse the frequency spectrum. The reuse of the frequency spectrum requires that there are multiple cells transmitting on the same frequency band. In TDMA cellular systems, cells transmitting on the same frequency band are separated in space to minimize the effects of the interference due to sharing the frequency band (co-channel interference). CDMA uses a spreading signal to reduce the effects of co-channel interference. Each user is assigned a spreading signal that is approximately orthogonal to the other spreading signals. The desired signal is recovered by correlating the incoming signal with the spreading signal assigned to the user. The interference due to other uses is reduced in the correlation process and appears as noise to the receiver. The ability of CDMA to reduce the effects of co-channel interference allows for more users to transmit on the same frequency band at the same time.

Another advantage of CDMA is its soft capacity limit. The number of channels the frequency spectrum can be divided into limits analog, frequency-division systems; while the number of users per frequency channel for TDMA systems is limited by the number of timeslots the channel can be divided into. As the number of users in a CDMA system increases, the noise floor increases, degrading performance. Factors such as the power level and communication rate of other users determine the effect of other users on the noise floor, therefore, there is no absolute limit on the number of users in a CDMA system. The number of allowable users is a function of the system's ability to overcome noise generated by competing users.

The advantages of CDMA have made it the multiple access technique for the third generation of cellular phones. Initially, there was hope for a global 3G standard, but a worldwide standard has not materialized. W-CDMA and cdma2000 are competitors to become the 3G standard. Both systems promise data rates of 384kbs for mobile users and up to 2.4Mbs for stationary users. While proponents of W-CDMA and cdma2000 debate the merits of their systems as the standard for 3G cellular systems, companies have attempted to develop technologies to improve the performance and marketability of these systems. LinkAir is a company attempting to adapt new technology to cdma2000 to position itself in the 3.5G and fourth generation (4G) markets.

Attempting to improve the performance of cdma2000, LinkAir has developed LAS-CDMA. The benefit of LAS-CDMA technology comes from a new set of spreading codes. The new spreading codes of LAS-CDMA reduce the inter-symbol interference and multiple access interference to zero for all signals within an interference free time window. The interference free time window enables LAS-CDMA to have synchronous forward and reverse links. Synchronous forward and reverse links allow two-way communication on a single frequency band. This is an improvement over traditional wireless systems with asynchronous forward and reverse links that employ frequency division duplexing (FDD). In FDD systems two-way communication requires two frequency bands, one for transmitting and another for receiving. The FDD solution is conducive to situations such as voice communication, where the transmitted and received data rates are similar. Allowing for the dynamic allocation of code channels, LAS-CDMA can be adapted to both symmetric and asymmetric data rates. The ability to adjust

resources to varying data rates makes LAS-CDMA attractive for cellular technologies that will provide both voice and data services.

Besides new technology derived from new spreading codes, LinkAir's ability to enter the cellular market is also influenced by political considerations. The Chinese government's desire to use a Chinese cellular technology benefits LinkAir [8]. LinkAir's Beijing headquarters should help marketing LAS-CDMA to China, a huge potential market without a well-established cellular infrastructure. With the city government in Shanghai allowing LinkAir to test LAS-CDMA, it appears that LAS-CDMA has a market.

B. LAS SPREADING CODES

Many of the features of LAS-CDMA are made possible by using a new set of spreading codes. Superimposing two levels of codes, the LS and LA codes, forms the LAS spreading codes. The LAS spreading codes replace the Walsh codes that are used in other CDMA systems. Walsh codes are orthogonal when properly synchronized, but delays created by the multipath mobile environment introduce interference into the system. The LAS spreading codes create an interference free time window because LS codes combined with LA codes have the properties of orthogonal codes over the range of the window. The interference free time window allows LAS-CDMA to combat the delays introduced by the multipath mobile environment.

1. LS Codes

Channels within the cell are defined by the LS code assigned to it. The LS codes are formed in C and S component pairs. LS codes are 16,32,64, and 128 chips longs. The C and S components are transmitted in series. The C component is transmitted first and is preceded by a gap. The C component is separated from the S component by another gap. The gaps separating the C and S components are at least 4 chips in duration. The LA codes define the gap lengths. Using an LS code of length 128 chips results in a minimum LS code time interval of 136 chips. The structure of an LS code interval for a 128-chip LS code is shown in Figure 2.1.

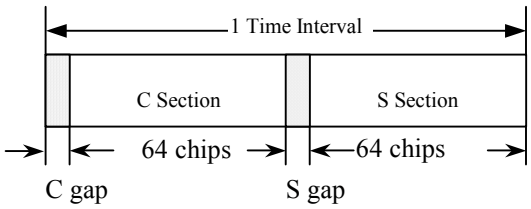

Figure 2.1. LS Code Structure. From Ref [9]

The correlation properties of spreading codes determine the capabilities of the code to separate channels in a cellular system. The LAS codes are designed to maximize the ability to separate cellular channels. The C and S components are such that the sum of the auto-correlations of any C and S component pair contains no side-lobes and the sum of the cross-correlation for any C components and any S components contains no side-lobes. The sum of the auto-correlations of a C and S component pair is defined as

$$R_{cs}(\tau) = R_c(\tau) + R_s(\tau) \tag{2.1}$$

where $R_c(\tau)$ is the auto-correlation of the C component and $R_s(\tau)$ is the auto-correlation of the S component. The sum of the C component cross-correlation and S-component cross correlation is defined as

$$R_{cs_i cs_j}(\tau) = R_{c_i c_j}(\tau) + R_{s_i s_j}(\tau) \tag{2.2}$$

where $R_{c_i c_j}(\tau)$ is the cross-correlation of two different C components and $R_{s_i s_j}(\tau)$ is the cross-correlation of two different S components. The sum of the auto-correlations for a pair of C and S components is shown in Figure 2.2. The sum of the cross-correlations of C and S components is shown in Figure 2.3.

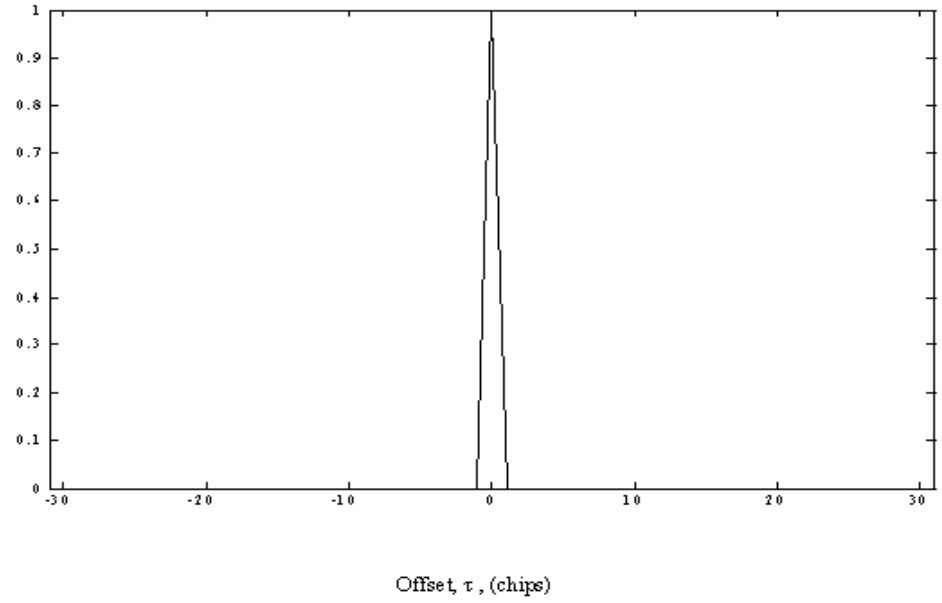

Figure 2.2. The Sum of the Auto-Correlations of an S and C component Pair.

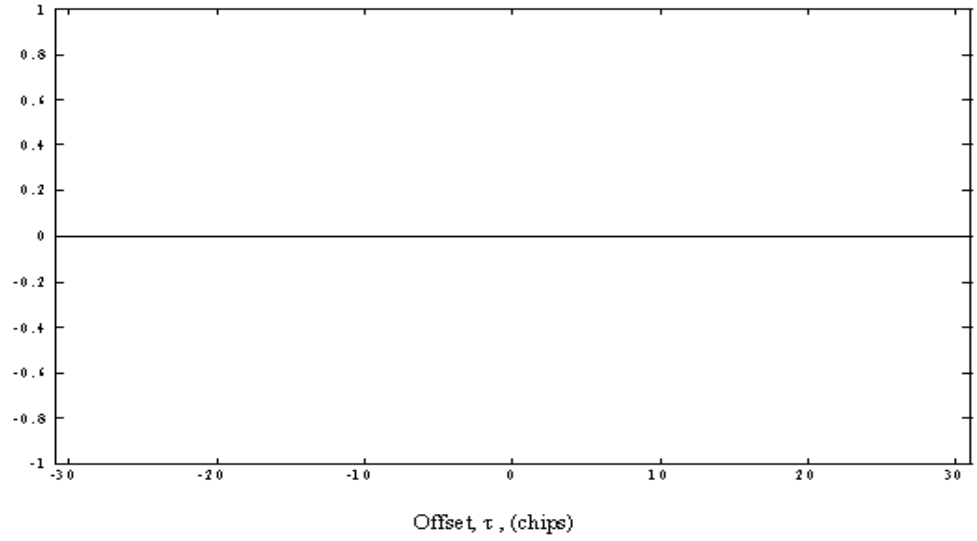

Figure 2.3. Sum of the cross-correlations of the C and S components

2. LA codes

Base stations are distinguished by their LA code. LA codes separate cells by randomizing the location of information bits in a packet. The LS code time intervals are separated by the LA code gaps of variable lengths. LAS-CDMA utilizes a set of LA codes

that combine 17 LS code time intervals into a 2559-chip sequence. LAS-CDMA utilizes a set of 16 possible LA codes. These codes were found by computer search and combined with the LS codes they yield an interference free time window [10].

The LA codes are a series of intervals of variable lengths. The 17 LS code intervals that form the time intervals are given a length index. The length index determines the length of the LS code gaps and length of the LA code interval. The LA code is generated by transmitting the LS code intervals according to the length index number. Table 2.1 defines the LS gap lengths for the LA code used in LAS-CDMA. The lengths of the individual LA code intervals are defined in Table 2.2. The set of 16 LA codes used in LAS-CDMA are defined in Table 2.3.

Table 2.1. Length of LS Code Gaps. From Ref [9].

Length Index	1	2	3	4	5	6	7	8	9	10	11	12	13	14	15	16
CGap (chips)	4	5	6	7	8	9	10	11	12	13	14	15	16	17	18	4
SGap (chips)	4	5	6	7	8	9	10	11	12	13	14	15	16	17	18	5

Table 2.2. Lengths of the LA Code Time Intervals Used by LAS-CDMA. From Ref [9].

	Interval Sequence in the Primary LA Code																
Length Index	0	1	2	3	4	5	6	7	8	9	10	11	12	13	14	15	16
Length (chips)	136	138	140	142	144	146	148	150	152	154	156	158	160	162	164	172	137

Table 2.3. Set of LA Codes Used by LAS-CDMA. From Ref [9].

LA Code Permutation Index	Time Interval Sequence of LA Codes																
0	0	1	2	3	4	5	6	7	8	9	10	11	12	13	14	15	16
1	0	2	4	6	8	10	12	14	16	1	3	5	7	9	11	13	15
2	0	3	6	9	12	15	1	4	7	10	13	16	2	5	8	11	14
3	0	4	8	12	16	3	7	11	15	2	6	10	14	1	5	9	13
4	0	5	10	15	3	8	13	1	6	11	16	4	9	14	2	7	12
5	0	6	12	1	7	13	2	8	14	3	9	15	4	10	16	5	11
6	0	7	14	4	11	1	8	15	5	12	2	9	16	6	13	3	10
7	0	8	16	7	15	6	14	5	13	4	12	3	11	2	10	1	9
8	0	9	1	10	2	11	3	12	4	13	5	14	6	15	7	16	8
9	0	10	3	13	6	16	9	2	12	5	15	8	1	11	4	14	7
10	0	11	5	16	10	4	15	9	3	14	8	2	13	7	1	12	6
11	0	12	7	2	14	9	4	16	11	6	1	13	8	3	15	10	5
12	0	13	9	5	1	14	10	6	2	15	11	7	3	16	12	8	4
13	0	14	11	8	5	2	16	13	10	7	4	1	15	12	9	6	3
14	0	15	13	11	9	7	5	3	1	16	14	12	10	8	6	4	2
15	0	16	15	14	13	12	11	10	9	8	7	6	5	4	3	2	1

The LS code and LA code are combined by inserting LS code segments into the variable length LA code intervals. The lengths of the LS gaps are determined by the length index of the LA code interval that the LS code segment is being inserted into. Table 3 defines the sequence of length indexes for LA codes used in LAS-CDMA. Table 2 defines the length of the LS gaps for the length indexes. The length of LA gap at the end of the LA time interval is determined by the length index and length of the LS code. The length of the LA gap is adjusted so that the LA code interval is the length prescribed by the length index. The structure for inserting the LS code segments into LA code intervals is shown in Figure 1.4. By using a set of LA codes with LS gaps of at least four chips, LAS-CDMA is assured of having an interference free time window of at least nine chips in duration. The interference free time window is shown in Figure 2.5 and Figure 2.6. Figure 2.5 shows the interference free time window in the auto-correlation of the LAS spreading code. Figure 2.6 shows the interference free time window in the cross-correlation of LAS spreading code.

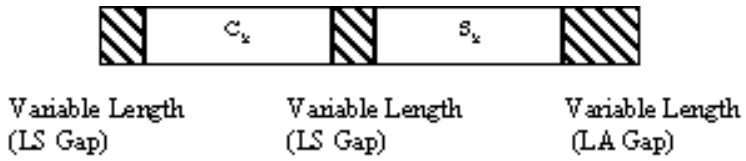

Figure 2.4. Structure of LS and LA Code Combination. From Ref [9].

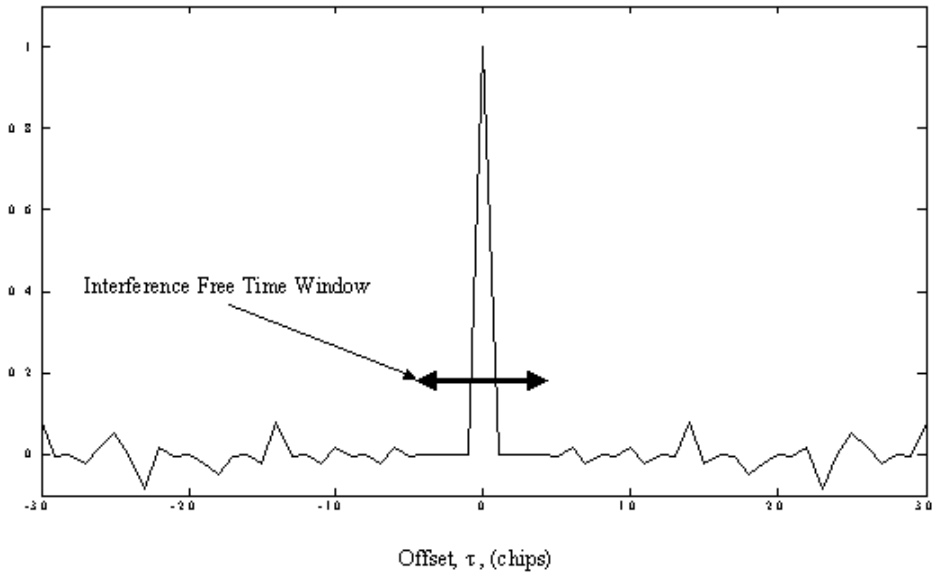

Figure 2.5. Interference Free Time Window in the Auto-Correlation of a LAS Spreading Code.

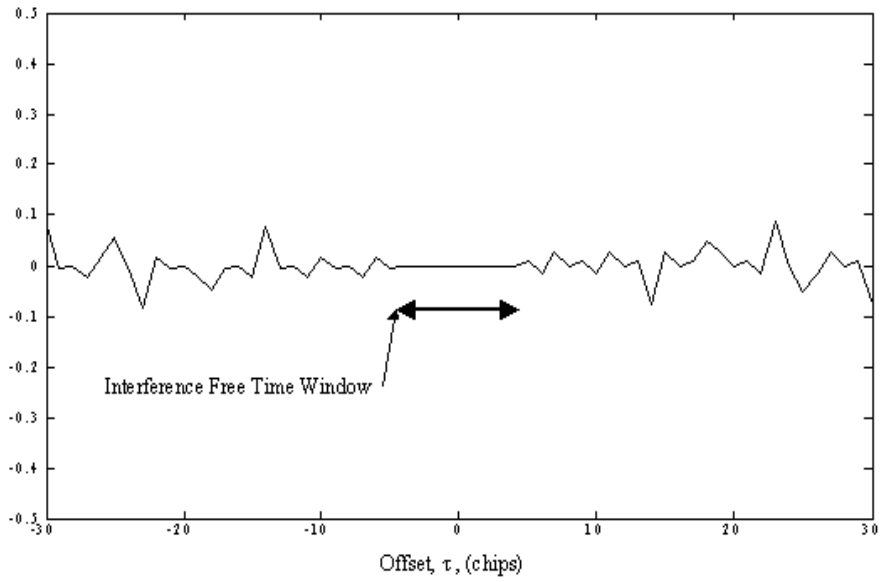

Figure 2.6. The Interference Free Time Window in the Cross-Correlation of the LAS Spreading Code.

The combination of LS and LA codes give LAS-CDMA several desirable characteristics. The interference free time window produced by the LS and LA codes improves the capacity of LAS-CDMA by reducing interference. Interference limits the number of users of previous CDMA systems, including cdma2000. Strategies to increase the capacity of CDMA systems by minimizing the effect of interference have been developed. The "near-far" effect can be disastrous for CDMA systems. The "near-far" effect happens because, if all mobile stations transmitted at the same power, more energy from the signal transmitted by a mobile station close to the base station would be received than from a signal transmitted by a mobile unit near the cell boundary. The non-synchronous reverse link on previous CDMA systems was particularly susceptible to interference. To minimize the effect of the interference, CDMA systems utilized power control features to equalize the strength of the signals received at the base station. The synchronous reverse link and interference free time window makes LAS-CDMA unaffected by the "near-far" effect. LAS-CDMA does incorporate less responsive power control to maximize battery life.

LAS-CDMA spreading codes also reduce the benefit of the use of smart antennas. Smart antennas reduce interference by using beam forming techniques to reduce co-channel interference via spatial filtering. With the spreading codes eliminating the multiple access interference within the interference free time window, the benefit of using a smart antenna is greatly reduced.

As well as improving the ability to reject interference from other users, LAS-CDMA spreading codes also help reject intersymbol interference. Intersymbol interference is caused by multipath propagation that can lengthen the time required to receive the signal. The delay causes energy from the previous symbol to bleed into the next symbol. The auto-correlation of the LAS spreading code, shown in Figure 2.5, illustrates how the LS spreading works to reduce the interference caused by a multipath propagation delay of less than one chip duration and eliminates interference caused by a multipath propagation delay within the range of the interference free time window but greater than one chip duration.

C. ERROR CORRECTION CODING

Error correction coding has made digital communications practical and popular. Unlike analog systems, digital systems can detect and correct errors. Transmitted signals are coded to improve the ability of the receiver to recover the original data. The codes used in communication systems are designed to combat the degenerative effects of the communication channel such as noise, interference, and fading. The trade-off for improved performance as result of the use of coding is increased redundancy. The added redundancy enables the receiver to detect and correct the errors caused by transmission, but also increases the bandwidth or decreases the data rate of the system. LAS-CDMA employs a cyclic redundancy check code, convolutional coding, interleaving, and symbol repetition to reduce the probability that a bit error occurs. The methods of error correction coding are described here. The effect of error correction coding is quantified in Chapter V.

1. Convolutional Coding

Convolutional codes encode a continuous stream of input information bits into a continuous stream of coded symbols. A convolutional code is described by the rate of the code, *k/n*, and the constraint length of the code, *K*. The rate of the code is also the amount of information contained in each coded bit. The constraint length represents the number of stages in the encoding shift register. The limitations of the decoder limit convolutional codes to constraint lengths no greater than nine. LAS-CDMA uses convolutional codes with a constraint length of nine and a variety of rates. The data rate and channel determines whether a convolutional code with rate 1/2, 2/3, or 3/4 will be used. To assist the decoding, a tail of eight zero-bits is added to the end of each data frame. These tail bits ensure that the encoder returns to the all zero state at the end of each data frame.

The convolutional codes selected for use in LAS-CDMA give the most error protection for a given rate and constraint length. The performance of a convolution code is related to the free distance of the code. As the free distance increases, the ability of the convolutional code to correct errors improves. For convolutional codes of a given constraint length, as the rate of the code decreases the free distance increases. Restricted to constrained length nine convolutional codes, to improve the probability of bit error LAS-CDMA must decrease the rate of the code or use a modulation technique that has better performance in the cellular channel.

2. Interleaving

Burst errors reduce the performance of convolutional codes. Burst errors are inevitable due to the nature of the wireless channel. Interleaving the coded data before it is transmitted randomizes the location of errors at the receiver. Interleaving is also used to obtain time diversity without added overhead.

Block interleaving with intercolumn permutations is utilized in LAS-CDMA. The block interleaver used on the LAS-CDMA Fundamental Channel formats 300 encoded data bits into a rectangular array of 10 rows and 30 columns. The size of the block

interleaver used on the LAS-CDMA Packet Data Channel varies in size from 64 bits to 16128 bits. The data bits are entered into the array by filling each row with successive bits from left to right. The method of filling the block interleaver is illustrated in Figure 2.7. The columns are shuffled in a predetermined fashion and the bits are read out of the interleaver from top to bottom, a column at a time. The method for reading bits out of the shuffled interleaver is illustrated in Figure 2.8.

$$\begin{bmatrix} u_1 & u_2 & u_3 & \dots\ u_{30} \\ u_{31} & u_{32} & u_{33} & \dots\ u_{60} \\ \vdots & \vdots & \vdots & \dots\ \vdots \\ u_{(R_2-1)30+1} & u_{(R_2-1)30+2} & u_{(R_2-1)30+3} & \dots u_{R_2 30} \end{bmatrix}$$

Figure 2.7. Order of Block Interleaver Input

$$\begin{bmatrix} y_1 & y_{R_2+1} & y_{2R_2+1} & \cdots y_{29R_2+1} \\ y_2 & y_{R_2+2} & y_{2R_2+2} & \cdots y_{29R_2+2} \\ \vdots & \vdots & \vdots & \dots\ \vdots \\ y_{R_2} & y_{2R_2} & y_{3R_2} & \cdots\ y_{30R_2} \end{bmatrix}$$

Figure 2.8. Order of Block Interleaver Output

3. Symbol Repetition

The symbol repetition employed by LAS-CDMA is a form of block error correction code. The repetition of symbols adds redundancy to the transmitted signal and improves the probability of the receiver correctly receiving the symbols. Depending on the channel and data rate, LAS-CDMA symbols are not repeated, repeated twice, repeated four times, or repeated eight times. As the number of repetitions increases, the number of errors that can be corrected also increases. The benefit of symbol repetition is dependent on the error correction methods employed by the receiver. The ability to correct errors with symbol repetition is quantified in Chapter V.

4. Cyclic Redundancy Codes

The Frame Quality Indicator is a cyclic redundancy code added to the Fundamental Channel. Cyclic redundancy codes are a linear class of error detecting codes that generate parity bits by finding the remainder of polynomial division. Cyclic redundancy codes are popular because the encoder and decoder are simple and they provide protection against burst errors. The ability of cyclic redundancy codes to detect errors improves as the number of redundant symbols sent increases [11]. LAS-CDMA increases the number of Frame Quality Indicator bits sent on the Fundamental Channel as the data rate increases and symbol repetition decreases.

5. Symbol Puncturing

Symbol puncturing allows convolutional codes rates to be adjusted without increasing the complexity of the decoder. The motivation for symbol puncturing in LAS-CDMA is to make the number of bits per frame constant rather than for error correction.

6. Turbo Codes

Turbo codes are parallel concatenated convolutional codes with a non-standard interleaver. The use of turbo codes requires the receiver to instantaneously determine the signal-to-noise ratio of the link. Turbo codes can achieve coding gains superior to other classes of error correction coding [7]. The implementation of turbo codes in LAS-CDMA is being studied. The turbo codes would replace the convolutional codes on the Packet Data Channel.

D. LAS-CDMA CHANNEL STRUCTURE

The LAS-CDMA Channel structure provides a format for the base station and mobile station to communicate. Communication requires that each coverage area include channels for traffic data and channels to manage the mobile users. Similar to other cellular systems, LAS-CDAM provides synchronization channels, pilot channels, access channels, and control channels. LAS-CDMA requires more timing control than previous

cellular systems to accommodate the synchronous forward and reverse channels. LAS-CDMA satisfies the expectations of 3G cellular systems with separate channels for voice traffic and data traffic. The LAS-CDMA reverse channel structure is illustrated in Figure 2.9. Figure 2.10 illustrates the forward channel structure.

The discussion of the LAS-CDMA channel structure here is limited to system timing, the Pilot Channel, the Fundamental Channel, and the Packet Data Channel. The Control Channel is included within the discussion of the Fundamental Channel and Packet Data Channel. The scope of the discussion of the Control Channel is limited to its interaction with the Fundamental Channel and Packet Data Channel. The Sync Channel is the topic of Chapter III. The Access Channel, Broadcast Channel, and Quick Paging Channel are outside the focus of this thesis and not discussed.

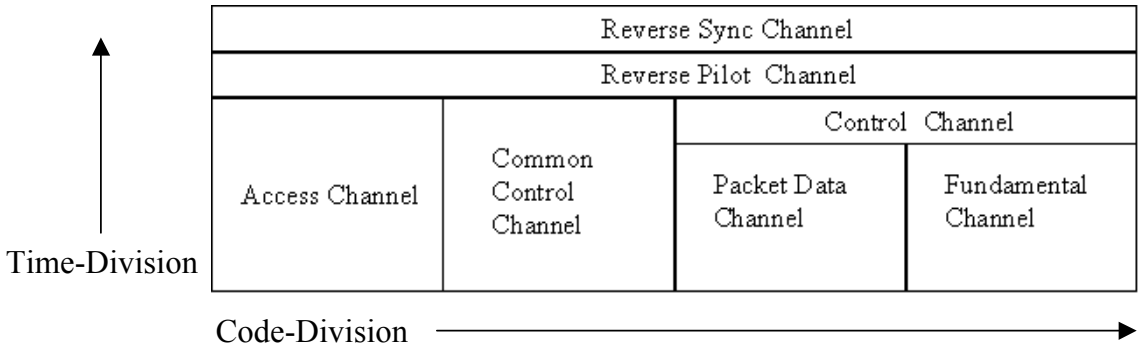

Figure 2.9. LAS-CDMA Reverse Channel Structure

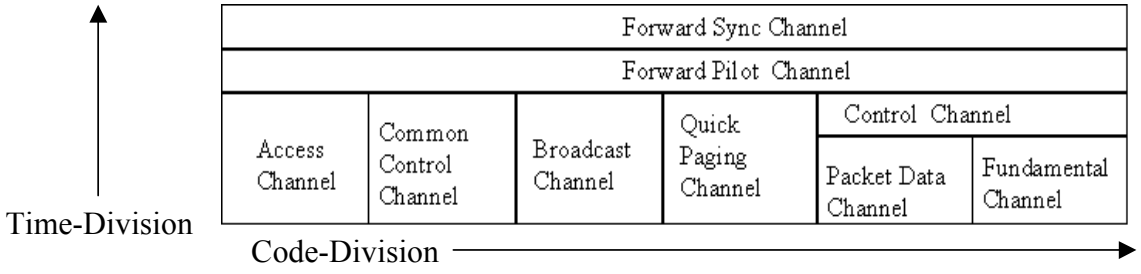

Figure 2.10. LAS-CDMA Forward Channel Structure

1. Timing

LAS-CDMA is designed to be compatible with IS-95 and cdma2000. Like IS-95 and cdma200, LAS-CDMA is spread at a chipping rate of 1.2288Mcps and is transmitted on a 1.25MHz bandwidth channel. The LAS-CDMA frame is 20ms in duration and contains 24576 chips. The frame is divided into eleven subframes. The first subframe contains 706 chips and transmits the Sync Channel. The other subframes each contain 2387 chips. The LAS-CDMA frame structure is shown in Figure 2.11. Each of the subframes $SF_1 - SF_{10}$ contains sixteen LA time intervals with an inserted LS code. The LA time intervals are of different lengths as specified by the LA code. The LAS-CDMA subframe structure is shown in Figure 2.12.

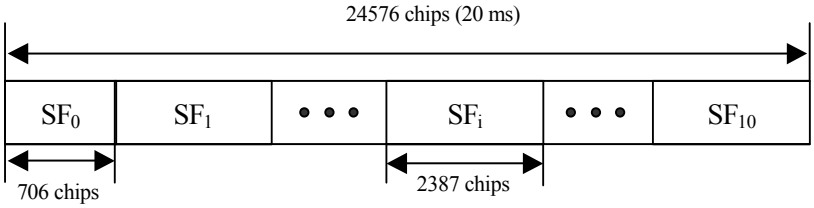

Figure 2.11. LAS-CDMA Frame Structure. From Ref [9].

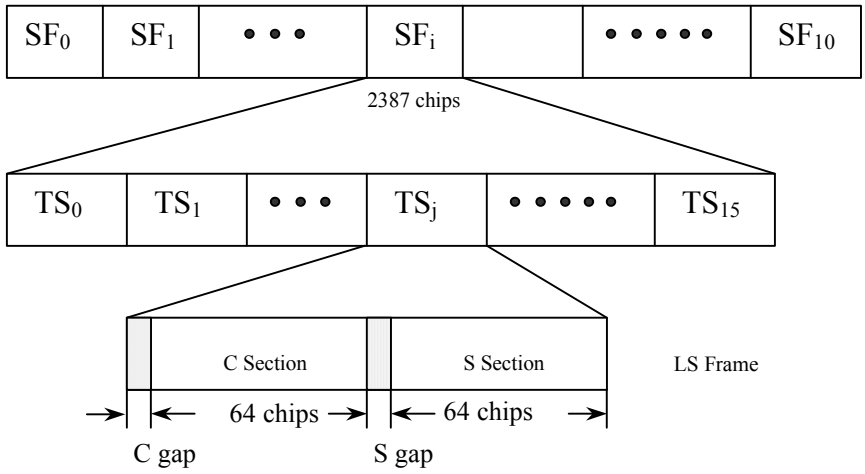

Figure 2.12. LAS-CDMA Subframe Structure For 128-Chip Length LS Code. From Ref [9].

Unlike previous cellular technologies, the forward and reverse LAS-CDMA channels are synchronous. The LAS-CDMA spreading codes are orthogonal if the delay between users is within the range of the interference free time window. LAS-CDMA synchronous reverse link takes advantage of the ability of the mobile stations to be synchronized within the interference free time window.

To help with the synchronization of the mobile stations and surrounding cells, LAS-CDMA utilizes a system-wide time scale based on the GPS time scale. LAS-CDMA system time is referenced to the same start as GPS, January 6, 1980 00:00:00. The first chip of the LAS-CDMA Forward Channel frame is transmitted starting at an instant in time that an integer number multiple of 20ms time frames from the start of system time.

To maintain a synchronous reverse channel with orthogonal spreading codes, the LAS-CDMA mobile station is required to maintain two time references, one for the forward link and one for the reverse link. The forward time reference is established according the received frames of the Forward Sync Channel. To maximize the interference rejection capabilities, all multipath components must be received by the mobile station within the interference free time window. To time the interference time window for maximum interference rejection, the forward time reference is required to be

able to estimate the arrival of the first multipath component of the transmitted signal within one millisecond. The forward time reference is used as the initial reverse time reference. After the initial forward time reference is established, the base station instructs the mobile station to adjust the forward time reference for optimal interference rejection at the base station.

2. Pilot Channel

LAS-CDMA uses modulation techniques that require coherent detection. Coherent modulation techniques allow LAS-CDMA to increase the data rate without increasing the symbol rate. Coherent detection requires that a pilot tone be sent so that the receiver can be phase-synchronized with the received signal. LAS-CDMA uses a burst pilot to provide the phase synchronization required for coherent detection. Coherent detection at both the base station and mobile station requires that the Burst Pilot Sub-Channel be included in both the forward and reverse link. The Burst Pilot Sub-Channel is transmitted on the first LA time interval of the LAS-CDMA subframes SF_1 through SF_{10}. The timing characteristics of the Burst Pilot Sub-Channel are illustrated in Figure 2.13. Each Pilot burst is 128 chips in duration. The Burst Pilot Sub-Channel transmits a '0' symbol for the duration of the 128 chips. The Burst Pilot Sub-Channel is modulated and spread using the same modulation scheme and spreading code used in the associated channel.

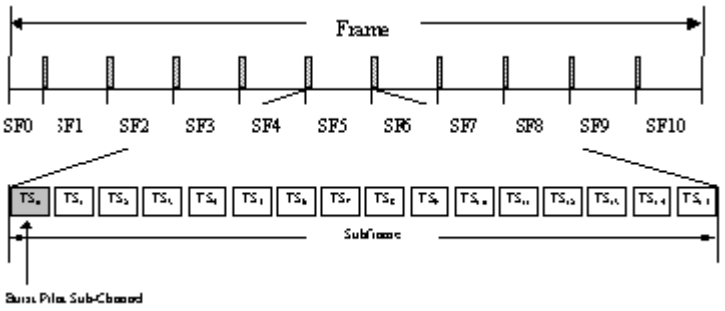

Figure 2.13. Burst Pilot Timing. From Ref [9].

3. Fundamental Channel

The Fundamental Channel is the LAS-CDMA channel designated for voice traffic. A 16-QAM, encoded, spread spectrum signal is used to transmit the voice traffic on the Fundamental Channel. The Fundamental Channel is spread by a 128-chip length LS code and the LA code assigned to the coverage area.

The Fundamental Channel can operate in two possible radio configurations, Radio Configuration 1 (RC1) and Radio Configuration 2 (RC2). These radio configurations are adapted from cdma2000 radio configurations. The symbol rate is constant within each of the radio configurations. Symbol repetition is used to hold the symbol rate constant. The radio configurations are assigned so that a mobile station supporting Radio Configuration 1 on the forward link will support Radio Configuration 1 on the reserve link. The data rate and properties of Radio Configuration 1 are listed in Table 2.4 and the data rate and properties of Radio Configuration 2 are listed in Table 2.5.

Table 2.4. Properties of Radio Configuration 1. After Ref [9].

	Data Rate (bps)				
Parameter	**10000**	**5000**	**2500**	**1300**	**Units**
Chip Rate	1.2288	1.2288	1.2288	1.2288	Mcps
LA code	(17, 136, 2559)				
LS code length	128	128	128	128	Chips
LS code gaps	Var+Var	Var+Var	Var+Var	Var+Var	Chips
Convolution Code Rate	2/3	2/3	2/3	2/3	bits/code symbol
Code Symbol Repetition	1	2	4	8	repeated code symbols per code symbol
Modulation Symbol Rate	8000	8000	8000	8000	Sps
Processing Gain	128	128	128	128	chips/bit

Table 2.5. Parameters For Radio Configuration 2. After Ref [9].

	Data Rate (bps)				
Parameter	**15000**	**7500**	**3800**	**1,900**	**Units**
Chip Rate	1.2288	1.2288	1.2288	1.2288	Mcps
LA code	(17, 136, 2559)				
LS code length	128	128	128	128	Chips
LS code gaps	Var+Var	Var+Var	Var+Var	Var+Var	Chips
Convolution Code Rate	2/3	2/3	2/3	2/3	bits/code symbol
Code Symbol Repetition	1	2	4	8	repeated code symbols per code symbol
Modulation Symbol Rate	11820	11820	11820	11820	Sps
Modulation Symbol Duration	84.6	169.2	334	668	μs
Processing Gain	128	128	128	128	chips/bit

The Fundamental Channel transmits using the LAS-CDMA frame structure and is time division multiplexed with the Sync Channel, the Burst Pilot Sub-Channel, and a Power Control Channel. The Sync Channel is transmitted in the first subframe, SF_0. The Burst Pilot Sub-Channel and Power Control Channel are transmitted on the first two LA code time intervals of the other subframes, $SF_1 - SF_{10}$. The Fundamental Channel frame structure is shown in Figure 2.14.

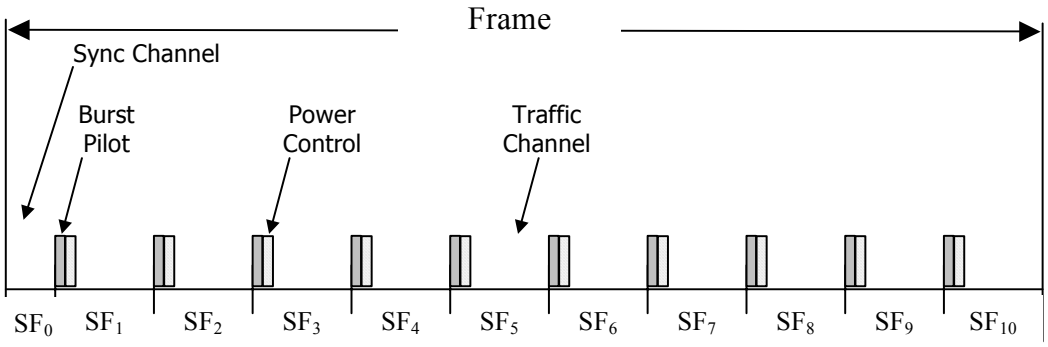

Figure 2.14. Fundamental Channel Frame Structure. From Ref [9].

a. Reverse Fundamental Channel

The Reverse Fundamental Channel supports voice communications from the mobile station to the base station. A combination of encoded data bits, power control bits, frame quality indicator bits, and padded bits are modulated into 16-QAM symbols to form the Reverse Fundamental Channel symbols. The transmitter for the Reverse Fundamental Channel is illustrated in Figure 2.15. As illustrated in Figure 15, the Reverse Fundamental Channel incorporates a combination of error correction techniques to reduce the probability of bit error. The Reverse Fundamental Channel uses the frame quality indicator, rate 2/3 convolution coding, symbol repetition, and interleaving to reduce the bit error rate.

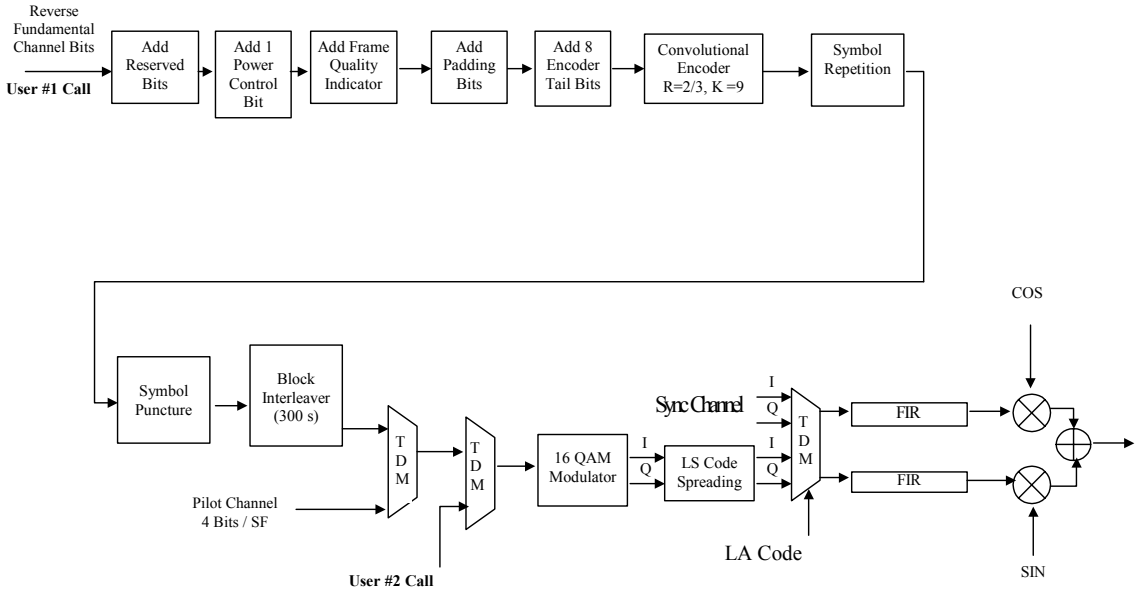

Figure 2.15. Reverse Fundamental Channel Transmitter. After Ref [9].

To increase channel capacity, the Reverse Fundamental Channel is time division multiplexed. Time division multiplexing two voice calls into the Fundamental Channel frame doubles the capacity of the Fundamental Channel. The first voice call, MS1, is transmitted in the odd subframes, $SF_1 - SF_9$, and the second voice call, MSC2, is

transmitted in the even subframes, $SF_2 - SF_8$. The structure of the multiplexed Fundamental Channel is illustrated in Figure 2.16. The time division multiplexing of the Reverse Fundamental Channel requires a high level of synchronization between the mobile stations and the base stations. The different propagation delays for different mobile stations have to be accounted for to ensure proper multiplexing of the received signals at the base station. The multiplexing of voice calls would appear to be a better strategy for the Forward Fundamental Channel. Mobile stations only need to know whether their message was sent in the even or the odd subframes rather than estimating the propagation delay.

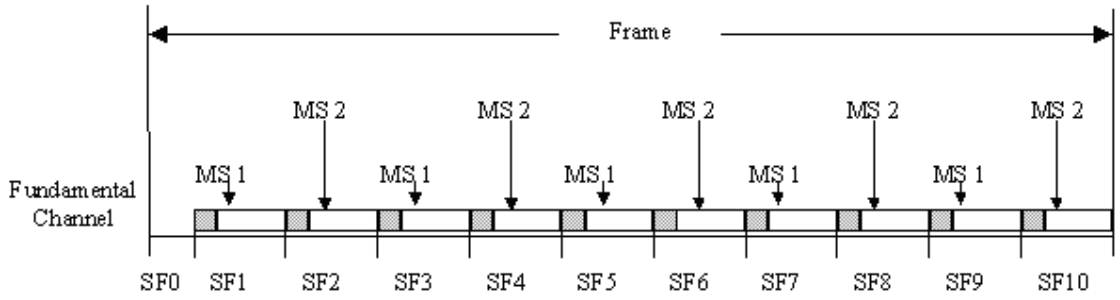

Figure 2.16. Reverse Fundamental Channel Frame Structure for Two Multiplexed Voice Calls. From Ref [9].

b. Forward Fundamental Channel

The Forward Fundamental Channel supports voice communications from the base station to the mobile stations. The Forward Fundamental Channel supports the same data rates as the Reverse Fundamental Channel. The characteristics of the Forward Fundamental Channel are similar to the Reverse Fundamental Channel. The block diagram of the transmitter for the Forward Fundamental Channel is illustrated in Figure 2.17. The data rates, convolutional code rate, signal modulation, and length of LS spreading codes are the same for both the Forward Fundamental Channel and the Reverse Fundamental Channel. Instead of time division multiplexing two voice calls onto one

channel like the Reverse Fundamental Channel, the Forward Fundamental Channel is used to transmit additional timing information to the mobile station.

In addition to the voice and error correction information transmitted on the Reserve Fundamental Channel, the Forward Fundamental Channel broadcasts two delay control bits in every frame. The Delay control bits are transmitted immediately following the power control bit. These bits help the mobile station to remain synchronous. The time adjustments are made in ¼-chip increments. The delay control bits will cause the mobile stations to advance ¼-chip, delay ¼-chip, or make no adjustment.

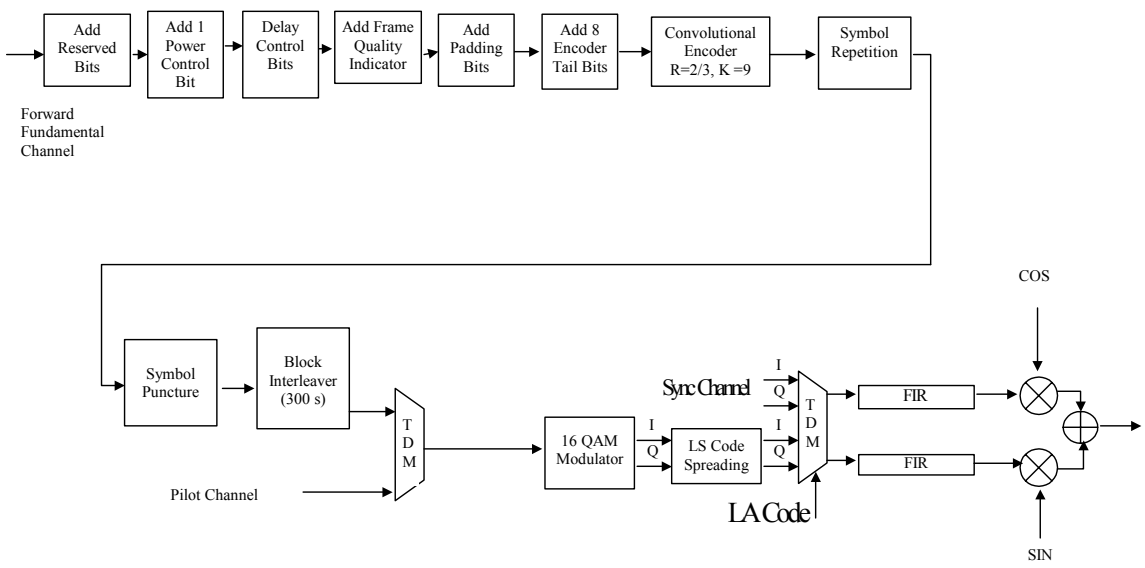

Figure 2.17. Forward Fundamental Channel Transmitter. After Ref [9].

4. Packet Data Channel

The Packet Data Channels are used to transmit high-speed packet data on the reverse and forward links. The Packet Data Channels are transmitted on the LAS-CDMA frame. Unlike the Fundamental Channel, the Packet Data Channel is unique to LAS-CDMA and is not based on cdma200 channels. The Packet Data Channel is time division multiplexed with the Sync Channel and transmits only in the subframes $SF_1 - SF_{10}$.

a. Reverse Fundamental Channel

The Reverse Packet Data Channel supports high-speed packet data communication from mobile station to the base station. The Reverse Packet Data Channel is designed to minimize interference, provide real time feedback control information for the Forward link, and to maximize the data rate. Depending on the desired data rate and channel conditions, the modulation technique, LS code length, and convolutional encoder rate of the Reverse Packet Data Channel are adjusted. The Reverse Packet Data Channel data rate defaults to 19.2 kbps and is adjusted depending on the channel conditions and amount of data to be sent. The Reverse Packet Data Channel parameters are listed in Table 2.6.

Table 2.6. Reverse Packet Data Channel Parameters. From Ref [9].

MCS Index	Data Rate (bps)	Packet Size (Bits)	Code Rate	Modulation Type	Modulation Symbols (sps)	LS Code Length
8	359700	7194	3/4	64 QAM	1600	8
7	179700	3594	3/4	64 QAM	800	16
6	57600	1152	3/4	16 QAM	400	32
5	38400	768	1/2	16 QAM	400	32
4	19200	384	3/4	8PSK	200	64
3	9600	192	1/2	QPSK	200	64
2	9600	192	3/4	8PSK	100	128
1	4800	96	1/2	QPSK	100	128

The Reverse Packet Data Channel is time division multiplexed with the Burst Pilot Sub-Channel, Reverse Common Control Channel, and Hybrid-ARQ Channel. The Burst Pilot Sub-Channel transmits in the first LA code interval of subframes $SF_1 - SF_{10}$ as discussed previously. The Hybrid-ARQ Channel transmits in the second LA code interval of subframes $SF_1 - SF_{10}$.

The Hybrid-ARQ Channel provides error control for the Forward Packet Data Channel. The Hybrid-ARQ Channel sends the base station a 1-bit indication of whether the mobile station has correctly received the previous subframe. Mobile stations send a positive or negative acknowledgment to the base station corresponding to each subframe. The base station transmits the next scheduled subframe if a positive acknowledgement is received. The current subframe is retransmitted if a negative acknowledgement is received or if no acknowledgement is received. The Hybrid-ARQ is only included on the reverse link. The forward link cannot request that the mobile resend the current subframe.

The mobile station use the Reverse Control Sub-Channel to inform the base station of the data rate, modulation techniques, and convolutional code rate used on the Reverse Packet Data Channel. The mobile station and base station use the control channels to estimate the channel characteristics and determine the modulation and code scheme (MSC). The Reverse Control Sub-Channel indicates the MSC for the current Reverse Packet Data frame and is transmitted in the third through sixth LA code time intervals of subframes $SF_1 - SF_{10}$. The MSC for the next Reverse Packet Data frame is transmitted on the Reverse Packet Data Rate Indication Sub-Channel in the seventh through tenth LA code time intervals of subframe SF_1. The MSC transmitted on the Reverse Packet Data Rate Indication Sub-Channel is translated and modulated by the same method as MSC transmitted on the Reverse Control Sub-Channel. The Reverse Packet Data Channel transmitter is illustrated in Figure 2.18. The structure of the Reverse Packet Data Channel is illustrated in Figure 2.19.

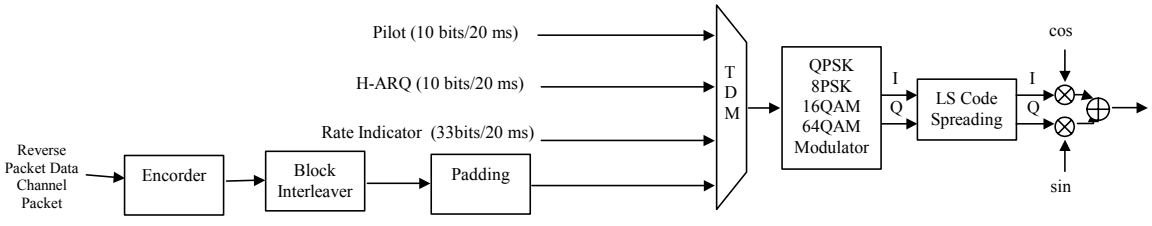

Figure 2.18. Reverse Packet Data Channel Transmitter. From Ref [9].

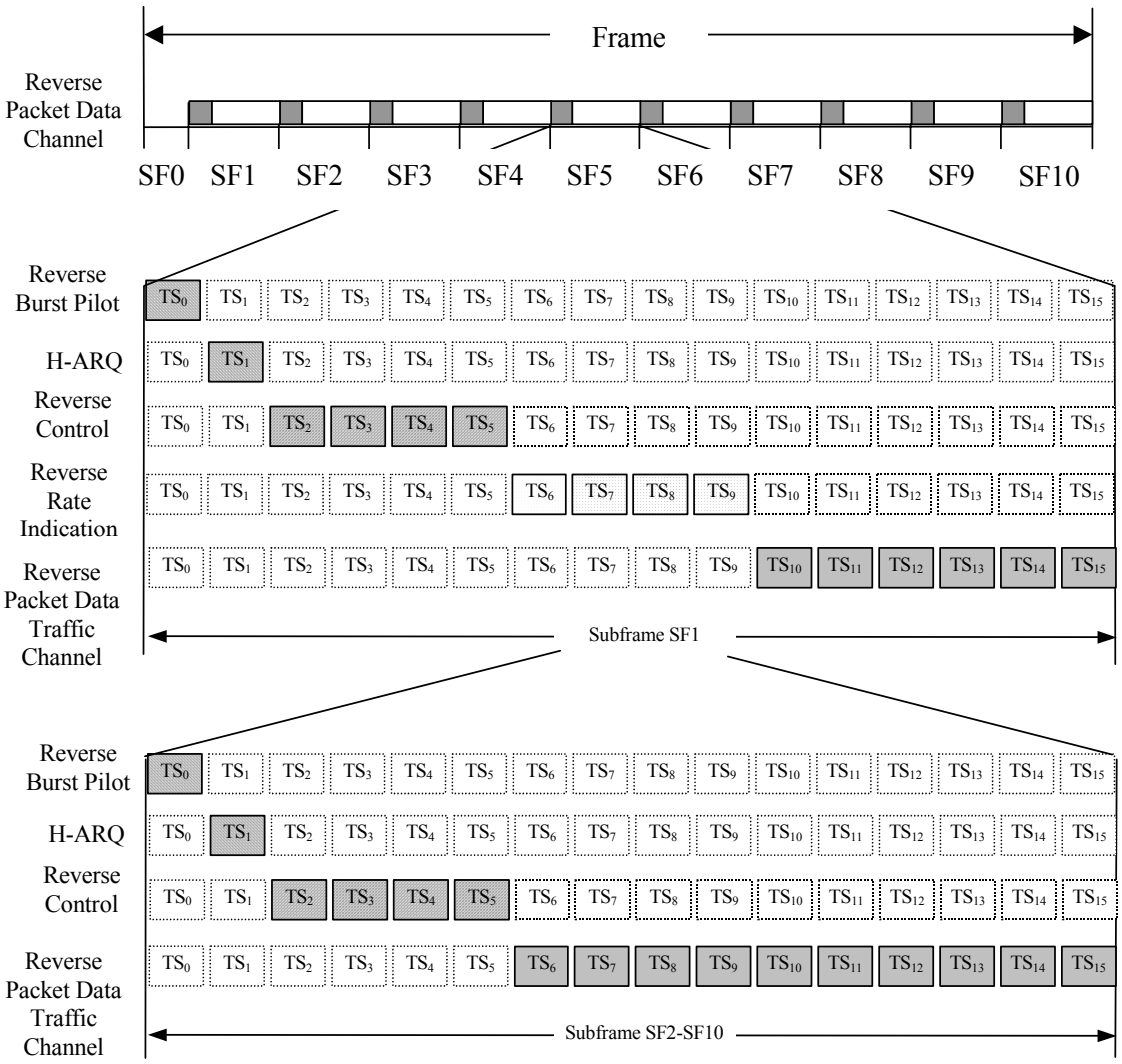

Figure 2.19. Reverse Packet Data Channel Subframe Structure. From Ref [9].

b. Forward Packet Data Channel

The Forward Packet Data Channel supports high-speed data transmission from the base station to the mobile station. Similar to the Reverse Packet Data Channel, the Forward Packet Data Channel can vary data rate by varying the modulation technique and coding rate. The Forward Packet Data Channel can also increase the data rate by assigning multiple code channels to a single mobile station. Depending on the traffic demands, the forward and reserve Packet Data Channels can adjust from two to 14 orthogonal LS code channels. The data is spread with 16-chip length LS codes that form

the orthogonal LS code channels. The data rates, modulation techniques, and coding rates for the individual Forward Packet Data Channel are listed in Table 2.7.

Table 2.7. Forward Packet Data Channel Parameters. From Ref. [9].

MCS Index	Data Rate (kbps)	Packet Size (Bits)	Code Rate	Modulation Type	Modulation Symbol Rate (ksps)	LS Code Length	LS Chips per Bit
8	216xN	432xN	3/4	64QAM	48xN	16	3.56
7	144xN	288xN	1/2	64QAM	48xN	16	5.33
6	144xN	288xN	3/4	16QAM	48xN	16	5.33
5	96xN	192xN	1/2	16QAM	48xN	16	8
4	108xN	216xN	3/4	8PSK	48xN	16	7.1
3	72xN	144xN	1/2	8PSK	48xN	16	10.67
2	60xN	120xN	3/4	QPSK	40xN	16	10.67
1	40xN	80xN	1/2	QPSK	40xN	16	16

N=2, 4, 6, 8, 10, 12

The Forward Burst Pilot Sub-Channel, Forward Control Channel, the Forward Packet Data Channel Preamble, and the Packet Data Traffic Channel are time division multiplexed on to the Forward Packet Data Channel. The structure of the Forward Packet Data Channel is illustrated in Figure 2.20. The Forward Control Channel transmits power adjustment, delay control, and rate control information from the base station to the mobile station. The preamble identifies the mobile station that the subframe is intended for. The ability to dynamically allocate subframes allows a single Forward Packet Data Channel to be shared by multiple mobile stations. The ability to divide the channel to match needs of the mobile stations makes the Forward Packet Data Channel more efficient.

The data rate of the Forward Packet Data Channel is adjusted using feedback from the mobile station. The Forward Rate Control bits transmitted by the mobile station are determined by the estimate of the channel conditions by the mobile station. The Forward Rate Control informs the base station of the optimal data rate the mobile station is capable of receiving. The base station considers the Forward Rate Control and system load for the coverage area and determines the data rate for the

Forward Packet Data Channel. An overhead control channel broadcasts the data rate of the next Forward Packet Data Channel frame.

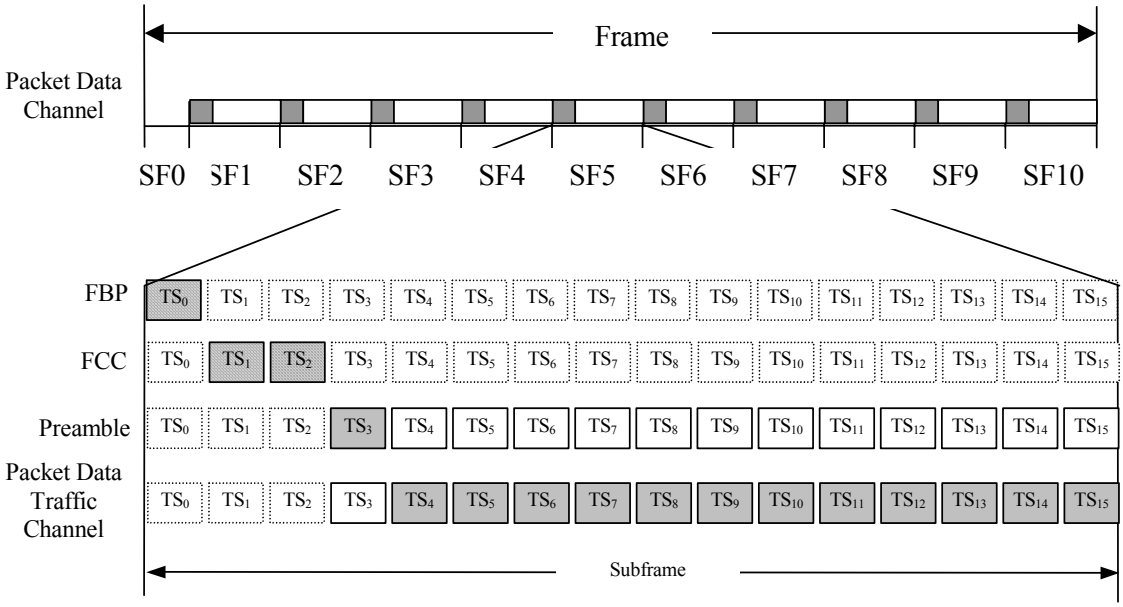

Figure 2.20. Forward Packet Data Channel Structure. From Ref [9].

THIS PAGE INTENTIONALLY LEFT BLANK

III. SPREADING CODE SYNCHRONIZATION

A. INTRODUCTION

CDMA systems use spreading codes to separate users in the wireless channel. The spreading codes reduce interference between users, but also increase the difficulty of receiving the signal. To receive the signal, the receiver must know the spreading code used to spread the received signal and be correctly synchronized in time with the received signal. LAS-CDMA, like other CDMA systems, broadcasts a synchronization (Sync) channel to assist the mobile station with synchronizing with the base station. While the Sync Channel assists the process of synchronizing for the intended recipient, unintended recipients can also use the Sync Channel for synchronizing and intercepting LAS-CDMA signals. This chapter will examine the LAS-CDMA Sync Channel, methods of synchronizing with the signal, and security issues with LAS-CDMA.

B. SYNC CHANNEL

The Sync Channel is an encoded, interleaved, modulated spread spectrum signal. The Sync Channel is transmitted in the first subframe of every 20 ms, LAS-CDMA frame. Unlike clandestine spread spectrum systems which use a long, unpublished spreading code to increase the difficulty of intercepting the signal, LAS-CDMA increases the ease of synchronization by using short, published spreading codes. The Sync Channel is spread using the 32-chip LS spreading codes.

1. Forward Sync Channel

The Forward Sync Channel provides synchronization for the forward link and assists mobile stations with detecting forward link channels. It consists of ten Forward Sync Channel Slots and is preceded and followed by a 33-chip gap. Each Forward Sync Channel Slot contains one 32-chip LS code group. The structure of the Forward Sync Channel is illustrated in Figure 3.1.

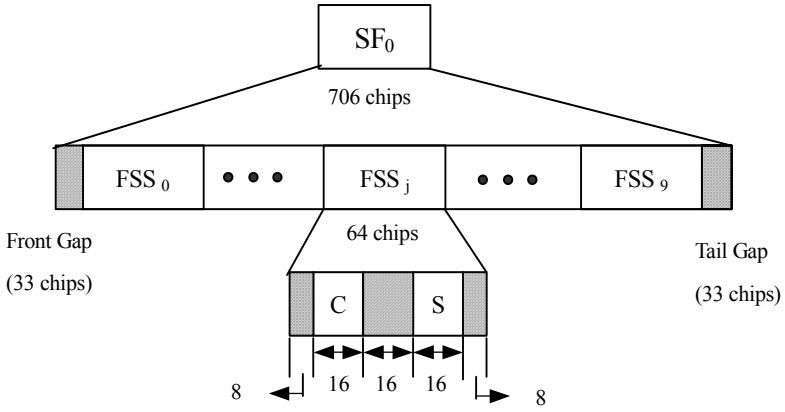

Figure 3.1. Forward Sync Channel Structure. After Ref [9].

The Forward Sync Channel is modulated using differential-quadrature phase shift keying (DQPSK). Although DQPSK does not perform as well as QSPK in AWGN, the ability to use noncoherent detection on DQPSK makes it more desirable for the Forward Sync Channel. DQPSK requires that a reference symbol be transmitted to initialize the demodulator. The first Forward Sync Channel symbol transmitted is the symbol '00'. The reference symbol is followed by an eight-bit unique word. The unique word is set to '11100101'. After the unique word the Forward Sync Channel broadcasts a four-bit LA code index and a four-bit LS code group index. The LA code index informs mobile stations of the LA code the base station is using to distinguish the coverage area. The set of LS codes used for the forward and reverse channels is specified by the LS code group index. The information structure of the Forward Sync Channel Frame is illustrated in Figure 3.2.

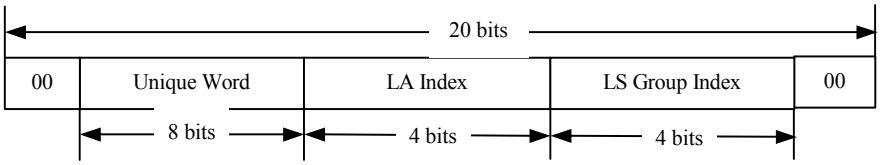

Figure 3.2. Forward Sync Channel Information Structure. From Ref [9].

The Forward Sync Channel is encoded using convolutional coding. The rate of the convolutional coding is determined by channel conditions. The rate 1/2 and rate 3/4 convolutional encoders that are used to encode the Forward Sync Channel are the same encoders used to encode the Packet Data Channel. The encoders are not reset between Forward Sync Channel Frames. The eight-bit unique word is used to initialize the decoder.

2. Reverse Sync Channel

The Reverse Sync Channel assists the base station with detection of the reverse link. The Reverse Sync Channel is divided into two to eight Reverse Synchronization Slots depending on the system configuration. A mobile station attempting to synchronize with a base station transmits a preamble in a Reverse Synchronization slot determined by the International Mobile Subscriber Identification number of the mobile station.

The base station receives the preamble from the mobile station and, by analyzing the arrival timing, decides if a delay adjustment is necessary. The base station sends the mobile station delay adjustment messages over the Access Delay Control Channel. The base station will send delay adjustments until the transmission timing is within a 1/4-chip range of the synchronization position.

C. SYNCHRONIZATION

One measure of the security of a cellular system is the ease with which unintended recipients are able to intercept the signal. Commercial CDMA systems must balance the

need for security with the ability for economical mobile stations to synchronize to the base stations. Unlike clandestine spread spectrum systems, which use a long, unpublished spreading code to increase the difficulty of synchronization, CDMA systems increase the ease of synchronization by using short, published spreading codes. This section will examine the ease with which LAS-CDMA can intercepted.

The Forward Sync Channel broadcasts information about the LA code and the LS codes used within the coverage area. If the Forward Sync Channel can be received, the receiver can use the information to receive other LAS-CDMA channels. To receive the Forward Sync Channel, the receiver must know the spreading code being used and be synchronized with the signal. We know that the Forward Sync Channel spreading code is formed by a 32-chip LS codes transmitted in the structure illustrated in Figure 3.1. We assume that all of the 32, 32-chip LS codes are equally likely. Also the center frequencies of 1.25MHz channels are assumed to be known and equally likely. Using knowledge of the spreading codes, we can examine methods of synchronizing with the received signal.

There are several techniques used to acquire synchronization. Synchronization techniques are evaluated by the average time required to synchronize with the received signal. The most common method is to search serially through all possible codes, code phases, and frequencies until the correct code, code phase, and frequency are found. This method is known as serial search. Pairing a specific 32-bit LS code and phase of the locally generated code forms search cells. To insure that the code is synchronized within a chip interval, the phase of the locally generated signal is incremented by half the chip duration. The serial search method generally assumes that all cells are equally likely [12]. If we assume all cells are equally likely, we are also making the assumption that the offset between the phase of the received code and the locally generated code is a uniformly distributed random variable.

The offset between the received Forward Sync Channel spreading code and the code generated to receive it can be modeled more accurately as a truncated Gaussian random variable. LAS-CDMA is designed to transmit the first chip of the Forward Sync Channel subframe at an integer multiple of 20 ms delay from the GPS reference time. When the code offset is not a uniform random variable, other search methods are more

efficient than the serial search technique. Evaluating the most likely cells before the less likely cells reduces the average synchronization time. We can assume that the offset between the received spreading code and the locally generated spreading code of the Forward Sync Channel follows a truncated Gaussian distribution. The standard deviation of the phase distribution does not affect the method of search. It is worth noting that as the standard deviation of the phase distribution increases the average synchronization time also increases. Cells are evaluated in discrete steps from the mostly likely cells to the least likely cells. This search technique is known as the z-search strategy [12]. The z-search strategy is illustrated in Figure 3.3.

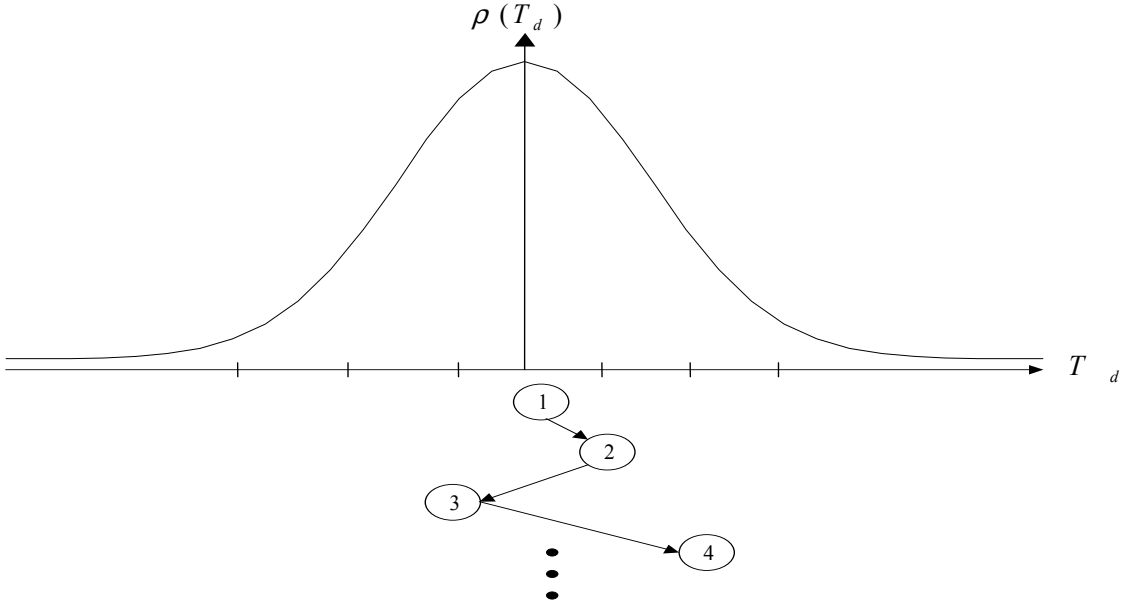

Figure 3.3. Z Search Strategy. After Ref [12].

Having selected a technique to evaluate cells, we need to specify how cells will be evaluated. The received Forward Sync Channel signal can be expressed as

$$r(t) = \sqrt{2}A_c c_i(t - T_d)\left(\cos\left(w_c t + \theta_m\right) + \sin\left(w_c t + \theta_m\right)\right) + n(t) \tag{3.1}$$

where $\sqrt{2}A_c$ is the amplitude of the received signal, $c_i(t)$ is the Forward Sync Channel spreading code where i is the index of the LS code used to generate the Forward Sync Channel spreading code, T_d specifies the phase of the received spreading code, θ_m is

determined by the DQPSK signal being transmitted, and *n(t)* is additive white Gaussian noise. The receiver must select the cell with the correct LS spreading code and the correct value of T_d in order to synchronize with the received code. Hypothesis testing tests the received signal with the search cells to determine which cell contains the correct LS spreading code and T_d. Assuming non-coherent detection of the Forward Sync Channel, the envelope detector illustrated in Figure 3.4 is the optimum detector to test the search cells [12]. The output of the envelope detector, Z, is compared to a threshold to determine whether the tested cell is correct. The envelope detector must be analyzed to select the desired threshold. The threshold is dependent on the desired probability of false alarm and probability of detection.

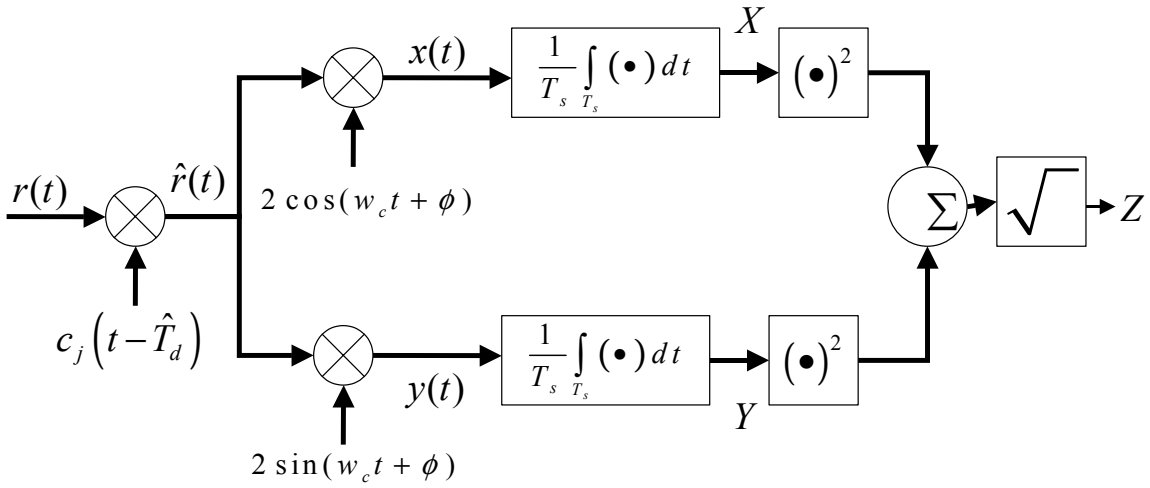

Figure 3.4. Envelope Detector. After Ref [12].

The distribution of Z when the correct cell is tested and the distribution of Z when the incorrect cell is tested are required to establish a decision threshold. If we assume the signal described by Equation 3.1 is received, the inputs to the integrators are

$$x(t)=\sqrt{2}A_c c_i(t-T_d)c_j(t-\hat{T}_d)\left[\cos(\phi-\theta_m)+\cos(2w_c t+\theta_m+\phi)+\sin(2w_c t+\theta_m+\phi)-\sin(\phi-\theta_m)\right]+n(t) \quad (3.2)$$

$$y(t)=\sqrt{2}A_c c_i(t-T_d)c_j(t-\hat{T}_d)\left[\sin(\phi-\theta_m)+\sin(2w_c t+\phi+\theta_m)+\cos(\phi-\theta_m)-\cos(2w_c t+\phi+\theta_m)\right]+n(t) \quad (3.3)$$

where $\hat{T}_d$ is the estimate of the phase of the received spreading code and ϕ is the phase of the detector. We assume the integrator eliminates the effect of the components at twice the carrier frequency. The output of the integrators can be modeled as Gaussian random variables with means given by

$$\bar{X} = \sqrt{2} A_c R_c \left(T_d - \hat{T}_d \right) \left[\cos(\phi - \theta_m) - \sin(\phi - \theta_m) \right] \tag{3.4}$$

$$\bar{Y} = \sqrt{2} A_c R_c \left(T_d - \hat{T}_d \right) \left[\sin(\phi - \theta_m) + \cos(\phi - \theta_m) \right] \tag{3.5}$$

where $R_c \left(T_d - \hat{T}_d \right)$ is the correlation function for the spreading code. The correlation function is given by

$$R_c \left(T_d - \hat{T}_d \right) = \frac{1}{T_s} \int_{T_s} c_i \left(t - T_d \right) c_j \left(t - \hat{T}_d \right) dt \, . \tag{3.6}$$

Figure 3.5 illustrates the correlation function when the received spreading code and the locally generated spreading code are the same. The correlation function when the received spreading code and locally generated spreading are different is illustrated in Figure 3.6. The variances of the Gaussian random variables that are used to model the output of the integrators are equal and are expressed as

$$\sigma_X^2 = \sigma_Y^2 = \frac{N_0}{T_s} \, . \tag{3.7}$$

The distributions of the Gaussian random variable at the integrator outputs are used to find the distribution of the envelope detector output.

To find the distribution of the detector output, it is necessary to make some assumptions. For the LAS-CDMA Forward Sync Channel, we can make the assumption that the correlation function is zero except when the locally generated spreading code and the received spreading code are the same and the offset between the spreading codes is less than one chip duration. From Figure 3.5 and Figure 3.6, we see that the spreading codes used to spread the Forward Sync Channel do not have side lobes within a 32-chip window centered on perfect synchronization. Using the GPS time reference to estimate the timing of the received signal, we can assume the detector will operate in the side lobe-free window. The simplified correlation function is given by

$$R_c(T_d - \hat{T}_d) = \begin{cases} 1 - \dfrac{\left|T_d - \hat{T}_d\right|}{T_c} & \textit{where} \quad \left|T_d - \hat{T}_d\right| < T_c \quad \textit{and} \quad i = j \\ 0 & \textit{otherwise} \end{cases} . \tag{3.8}$$

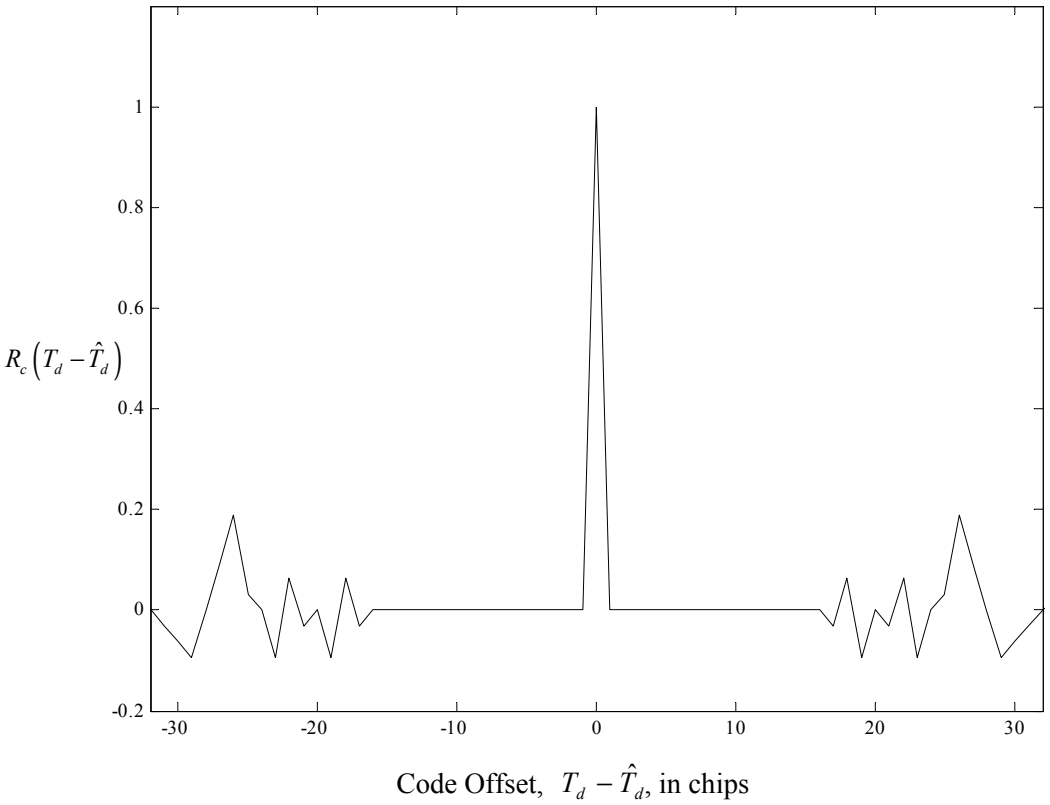

Figure 3.5. Cross-Correlation of the Received Spreading code and the Locally Generated Spreading Code when the LS Code of the Received Spreading Code and the LS code of the Locally Generated Spreading Code are the same.

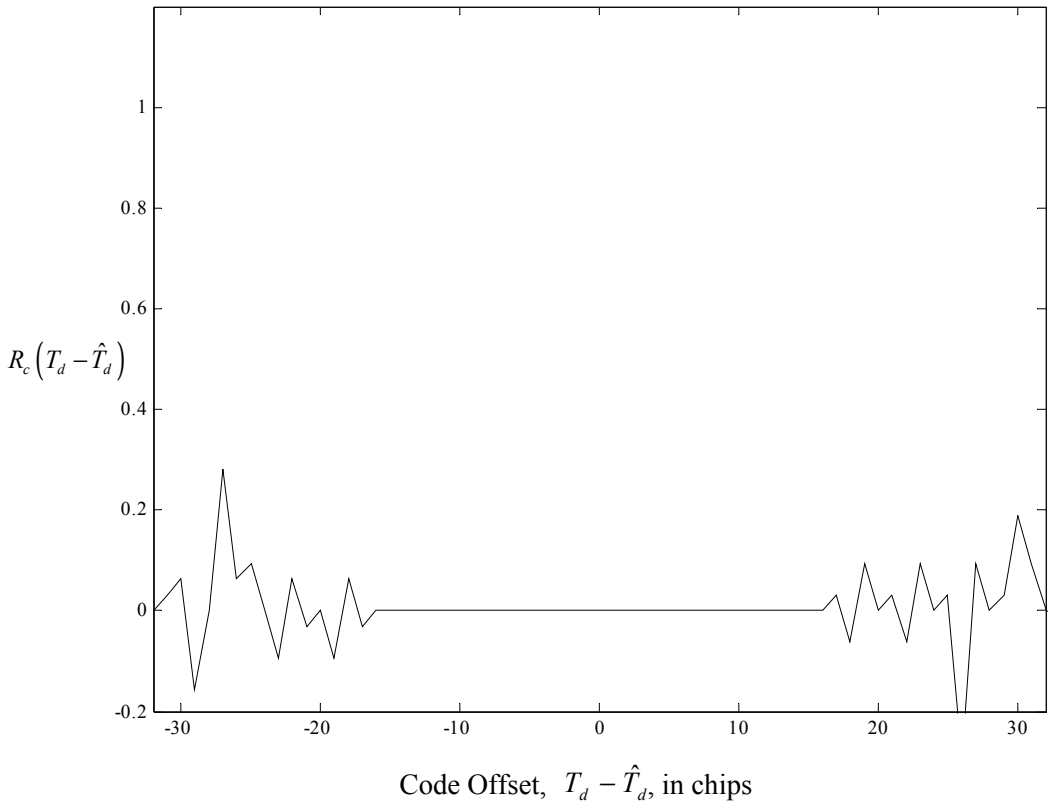

Figure 3.6. Cross-Correlation of the Received Spreading code and the Locally Generated Spreading Code when the LS Code of the Received Spreading Code and the LS code of the Locally Generated Spreading Code are Different.

Substituting the Equation 3.8 into Equation 3.4 and Equation 3.5 and performing a transformation of random variables to find the distribution of the envelope detector output, we see that the output of the detector is a Ricean random variable [12]. The distribution of the detector output is given by

$$f_Z(z)=\begin{cases}\dfrac{z}{N_0/T_s}e^{\frac{z^2+2A_c^2\left(1-\frac{T_d-\hat{T}_d}{T_c}\right)^2}{2N_0/T_s}}I_0\left(\dfrac{z\sqrt{2A_c^2\left(1-\dfrac{T_d-\hat{T}_d}{T_c}\right)^2}}{N_0/T_s}\right)U(z) & \text{when} \quad j=k \quad \text{and} \quad \left|T_b-\hat{T}_b\right|<T_c \\ \dfrac{z}{2N_0/T_s}e^{\frac{-z^2}{2N_0/T_s}}U(z) & \text{otherwise}\end{cases} \tag{3.9}$$

where $I_o(\bullet)$ is the zero-order, modified Bessel function and $U(\bullet)$ is the unit step function.

The analysis is simplified by assuming that when the correct cell is tested, $R_c\left(T_d - \hat{T}_d\right)$ is one and when the incorrect cell is tested, $R_c\left(T_d - \hat{T}_d\right)$ is zero. We can specify the distribution of the detector output conditioned on whether the cell being tested is the correct or incorrect cell. The distribution of the detector output given that the cell being tested in the correct cell is

$$f_Z(z\,|\,1) = \frac{z}{N_0/T_s} e^{-\frac{z^2+2A_c^2}{2N_0/T_s}} I_0\left(\frac{\sqrt{2}A_c z}{N_0/T_s}\right) U(z). \tag{3.10}$$

When the cell being tested is the incorrect cell, the distribution of the detector output is

$$f_z\left(z\,|\,0\right) = \frac{z}{N_0/T_s} e^{-\frac{z^2}{2N_0/T_s}} U(z). \tag{3.11}$$

The distribution of the detector output and the observed detector output are used to decide whether the cell being tested is the correct cell. The decision is made by comparing the probability of receiving the observed detector output assuming the tested cell is the correct cell with the probability of receiving the observed output assuming the tested cell is the incorrect cell. The decision rule is expressed as [13]

$$\frac{f_z\left(z\,|\,1\right)}{f_z\left(z\,|\,0\right)} \begin{array}{c} H_1 \\ > \\ < \\ H_0 \end{array} \lambda \tag{3.12}$$

where H_1 is the event of the correct cell, H_0 is the event of an incorrect cell, and λ is the threshold. A Neyman-Pearson philosophy should be used to set the threshold. The threshold is selected for Neyman-Pearson detector by designing for a desired probability of false alarm [13]. A Neyman-Pearson detector is suited for the synchronization circuit because it is desirable to design for a low probability of false alarm due to the time required to reject an incorrectly selected cell. The probability of false alarm is given by

$$P_{fa} = \int_{V_T}^{\infty} f_z\left(z\,|\,0\right) dz \tag{3.13}$$

where V_T is the threshold. The threshold also determines the probability of detection. The probability of detection is given by

$$P_d = \int_{V_T}^{\infty} f_z(z|1)\,dz\,. \tag{3.14}$$

Figure 3.7 illustrates the probability of false alarm and the probability of detection for a given signal power, noise power, and threshold.

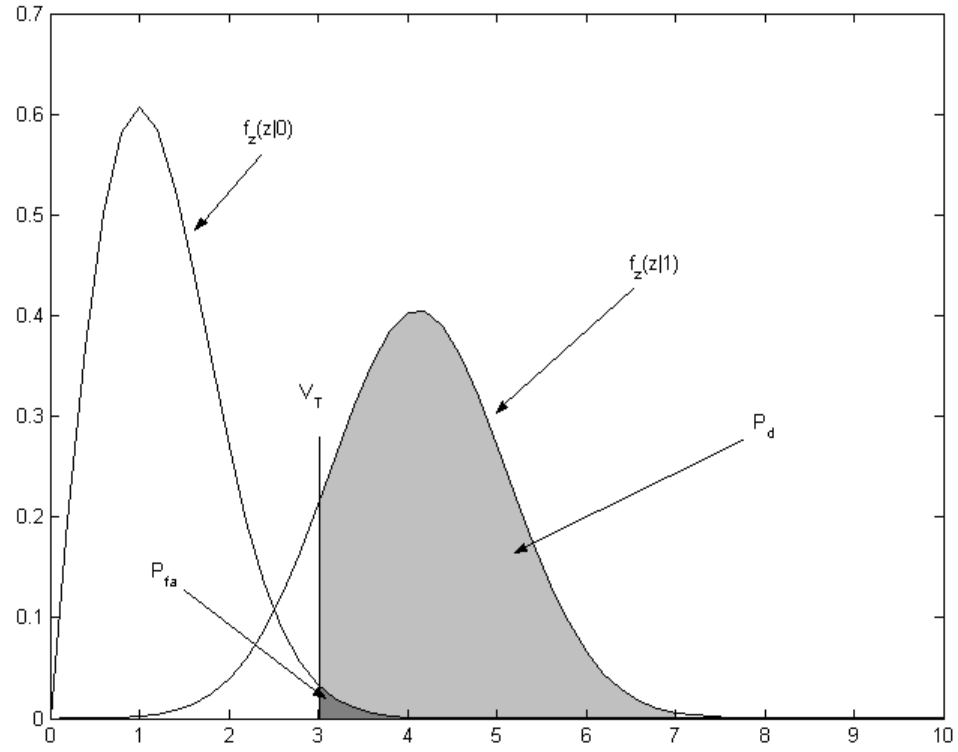

Figure 3.7. The Probability of False Alarm and the Probability of Detection For A_c^2=4, N_o=1, and V_T=3.

D. SECURITY

Once the LAS-CDMA Forward Sync Channel has been intercepted the other channels can be intercepted. The Forward Sync Channel broadcasts what codes will be used to spread the other channels. Other cellular communication standards use encryption

to add security to the traffic channels. IS-95 and cmda2000 encrypt the data transmitted by randomizing the data with a long PN sequence.

The long PN sequence is a period code that repeats approximately once a century. A 42-bit shift register is used to generate the PN sequence. Each IS-95 or cdma2000 user is assigned a unique generator seed during initialization [7]. Intercepting IS-95 or CDMA requires the receiver to synchronize with spreading codes and the PN sequence. To increase the difficulty of synchronizing with the long PN sequence, only one of every 64 PN sequence bits is used to scramble data [7]. Figure 3.8 illustrates a spread spectrum transmitter with data scrambling by a decided PN sequence.

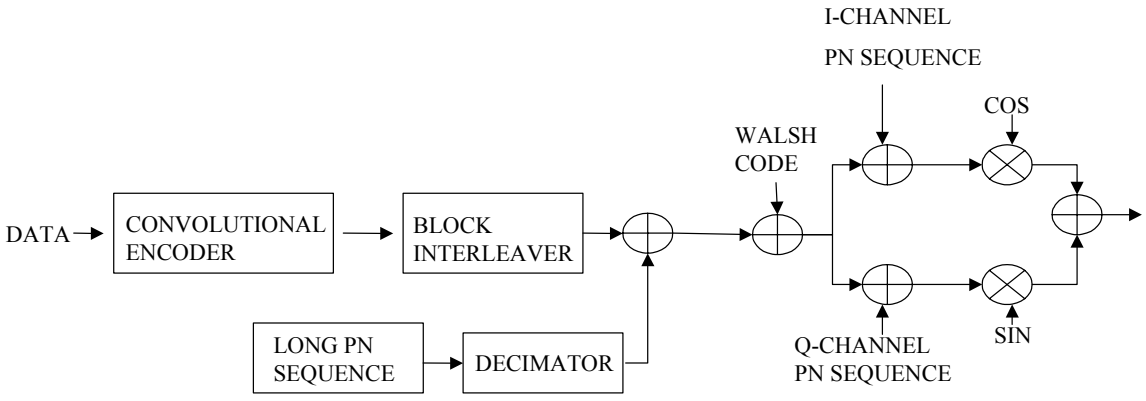

Figure 3.8. Spread Spectrum Transmitter with Data Scrambling. After Ref [7].

IV. ANALYSIS OF THE EFFECT OF A TONE JAMMER ON THE PERFORMANCE OF LAS-CDMA

A. TONE JAMMER

LAS-CDMA is designed to transfer information from one place to another. One figure of merit for LAS-CDMA is the probability of correctly communicating the message through a channel with noise and jamming. The transmission of a signal with the presence of a tone jammer in the wireless channel with AWGN is illustrated in Figure 4.1. The received waveform is represented by

$$r(t) = s_m(t) + s_j(t) + n(t) \tag{4.1}$$

where $s_m(t)$ is the message waveform, $s_j(t)$ is the waveform of the tone jammer, and *n(t)* is AWGN with a power spectral density of $N_o/2$.

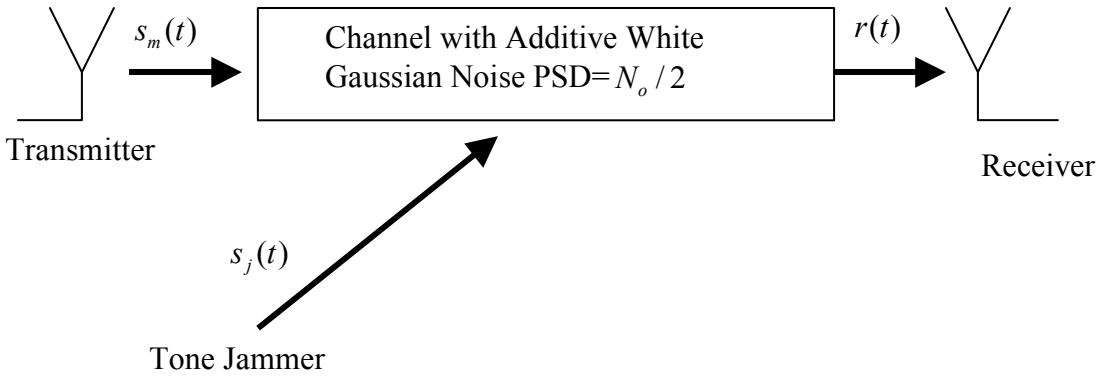

Figure 4.1 Wireless Channel With Tone Jammer.

A tone jammer is an unmodulated sinusoidal carrier. The tone jammer is important because it is easy to generate and is effective against direct-sequence spread spectrum signals. For maximum effect the tone jammer frequency should be the same as the carrier frequency of the transmitted signal [12]. Information about the spreading codes and modulation technique used by the attacked signal is not required. Only knowledge of the carrier frequency of the attacked signal is necessary. The tone jammer is represented by

$$s_j(t) = \sqrt{2}a_j \cos(w_c t + \theta_c) \tag{4.2}$$

where $\sqrt{2}a_j$ is the received amplitude of the jammer, w_c is the carrier frequency of the jammer, and θ_j is the phase of the tone jammer referenced to the phase of the attacked signal. This chapter will evaluate the probability of bit error for the modulation techniques and spreading rates used in LAS-CDMA for a Rayleigh fading channel with AWGN and a tone jammer.

B. PACKET DATA CHANNEL

The Packet Data Channel, as described in Chapter II, is designed to transmit high-speed data. The data rate is dependent on the MCS that determines the modulation technique and coding rate that will be transmitted. This section will examine the performance of the modulation technique and code rate combinations used on the LAS-CDMA Packet Data Channel. The modulation technique and coding rate combinations for the Packet Data Channel are listed in Table 4.1.

Table 4.1. Modulation and Code Pairs for the Packet Data Channel. After Ref [9].

MCS Index	Data Rate (kbps)	Code Rate	Modulation Type	LS Code Length
8	216xN	3/4	64QAM	16
7	144xN	1/2	64QAM	16
6	144xN	3/4	16QAM	16
5	96xN	1/2	16QAM	16
4	108xN	3/4	8PSK	16
3	72xN	1/2	8PSK	16
2	60xN	3/4	QPSK	16
1	40xN	1/2	QPSK	16

1. Quadrature Phase Shift Keying

The lowest data rates on the Packet Data Channel are transmitted using quadrature phase shift keying (QPSK). LAS-CDMA uses the QPSK signal constellation illustrated in Figure 4.2. The QPSK, spread spectrum signal can be expressed as [14]

$$s_{m,i}(t) = \sqrt{2}a_c c(t)\cos\left(w_c t - \frac{2\pi i + \pi}{4}\right) \quad \begin{matrix} 0 \le t \le T_s \\ i = 1,2,3,4 \end{matrix} \tag{4.3}$$

where $\sqrt{2}a_c$ is the amplitude of the received signal, *c(t)* is the LAS spreading code, and T_s is the symbol duration. The optimum demodulation of the QPSK, spread spectrum signal can be assumed because LAS-CDMA is a coherent system. The optimum demodulator uses in-phase and quadrature correlators to detect the phase angle of the received signal. Figure 4.3 illustrates the QPSK demodulator.

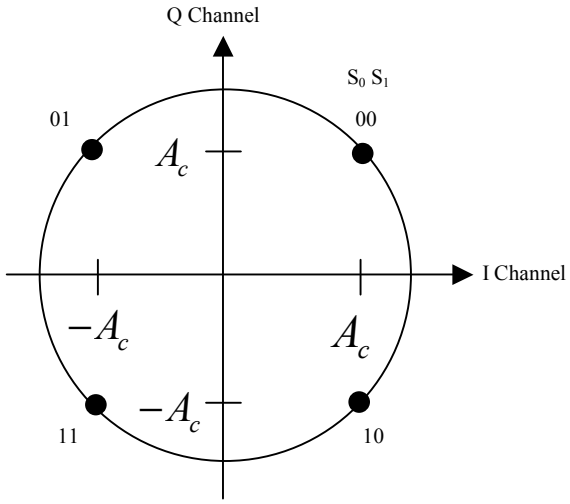

Figure 4.2. QPSK Signal Constellation. After Ref [9].

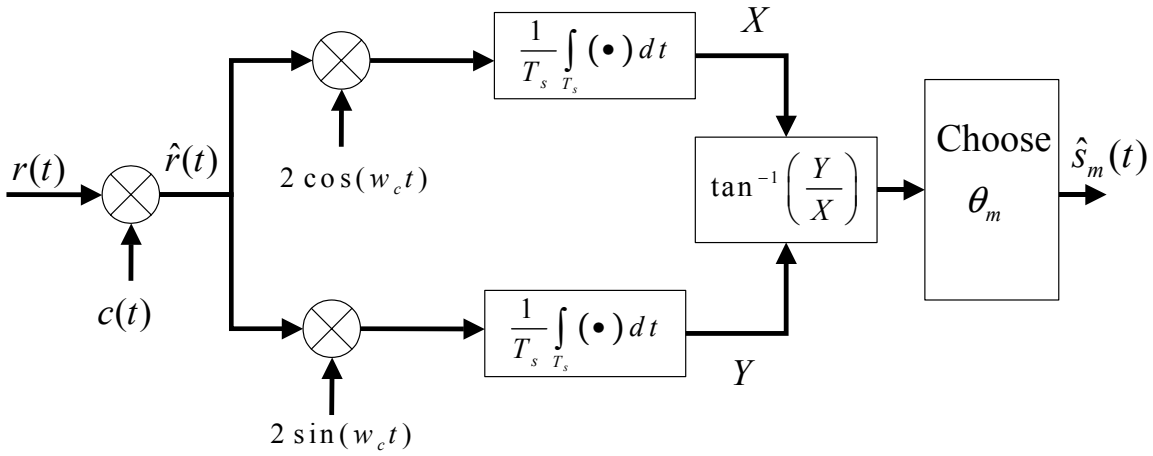

Figure 4.3. QPSK Demodulator. After Ref [14].

The received QPSK signal is expressed as

$$r(t) = \sqrt{2}a_c c(t)\cos\left(w_c t - \frac{2\pi i + \pi}{4}\right) + \sqrt{2}a_j \cos(w_c t + \theta_c) + n(t). \tag{4.4}$$

The received QPSK signal can be modeled as a gaussian random variable because the signal is the summation of the signal, the jammer, and AWGN. The outputs of the in-phase and quadrature correlators, X and Y, can also be modeled as Gaussian random variables because the inputs are Gaussian random variables and a Gaussian random variable multiplied by a scalar and integrated is also a Gaussian random variable. As Gaussian random variables, the correlator outputs are described by their mean and variance. The means of the correlator outputs are given by

$$\overline{X} = \pm a_c + a_j \cos(\theta_c) \cdot \frac{1}{T_s}\int_{T_s} c(t)dt \tag{4.5}$$

and

$$\overline{Y} = \pm a_c + a_j \sin(\theta_c) \cdot \frac{1}{T_s}\int_{T_s} c(t)dt. \tag{4.6}$$

The means of the correlator outputs can be simplified by accounting for the characteristic of the LAS spreading codes. The Packet Data Channel is spread by LS codes 16-chips in duration. A complete 16-chip LS code spreads each symbol. The integration of the spreading code over the symbol duration is

$$\frac{1}{T_s}\int_{T_s} c(t)dt = \frac{1}{16}\sum_{i=1}^{16} c_i \tag{4.7}$$

where c_i is the level of the i[th] chip. For LAS-CDMA, the level that *c(t)* can assume are limited to positive one and negative one. Given the possible levels of *c(t),* the integration of the spreading code over the symbol duration reduces to

$$\frac{1}{T_s}\int_{T_s} c(t)dt = \left(\frac{\rho}{8} - 1\right) \tag{4.8}$$

where ρ is the number of positive one chips in the spreading code. Substituting Equation 4.8 into Equations 4.5 and 4.6, we find the means of the correlator outputs are

$$\overline{X} = \pm a_c + a_j \cos(\theta_c) \cdot \left(\frac{\rho}{8} - 1\right) \tag{4.9}$$

and

$$\overline{Y} = \pm a_c + a_j \sin(\theta_c) \cdot \left(\frac{\rho}{8} - 1\right) \tag{4.10}.$$

The variances of the correlator outputs are expressed by

$$\sigma_X^2 = \text{var}\left[\frac{1}{T_s}\int_{T_s} 2\cos(w_c t)c(t)n(t)dt\right] \tag{4.11}$$

and

$$\sigma_Y^2 = \text{var}\left[\frac{1}{T_s}\int_{T_s} 2\sin(w_c t)c(t)n(t)dt\right] \tag{4.12}.$$

The variance of the correlator outputs is equivalent when the levels on *c(t)* are accounted for. The variance of the correlator outputs is

$$\sigma_X^2 = \sigma_Y^2 = \frac{N_o}{T_s} \tag{4.13}$$

where $\frac{1}{T_s}$ is the symbol rate.

An error occurs when the received signal is mapped to a point outside of the region assigned to the transmitted signal. QPSK transmits two bits in every symbol, so a symbol error may result in one or two bit errors. Gray coding maps bits to symbols so that the

most likely symbol errors will only result in one bit error. The probability of bit error for QPSK with gray coding given that the symbol '00' was sent is

$$\Pr[error \mid s_{00}] = \frac{\Pr[r_{01} \mid s_{00}]}{2} + \frac{\Pr[r_{10} \mid s_{00}]}{2} + \Pr[r_{11} \mid s_{00}] \tag{4.14}$$

where r represents the received symbol and s represents the transmitted symbol. The output of the correlators are Gaussian random variables with know means and variances. As a result, the probability of bit error given symbol '00' was transmitted is

$$\Pr[error \mid s_{00}] = \frac{1}{2}\left(1 - Q\left(\frac{\bar{X}}{\sigma_X}\right)\right)Q\left(\frac{\bar{Y}}{\sigma_Y}\right) + \frac{1}{2}\left(1 - Q\left(\frac{\bar{Y}}{\sigma_Y}\right)\right)Q\left(\frac{\bar{X}}{\sigma_X}\right) + Q\left(\frac{\bar{X}}{\sigma_X}\right)Q\left(\frac{\bar{Y}}{\sigma_Y}\right)$$

$$\Pr[error \mid s_{00}] = \frac{1}{2}Q\left(\frac{\bar{Y}}{\sigma_Y}\right) + \frac{1}{2}Q\left(\frac{\bar{X}}{\sigma_X}\right) \tag{4.15}$$

where

$$Q(z) = \int_z^\infty \frac{1}{\sqrt{2\pi}} e^{-\frac{x^2}{2}} dx .$$

Substituting the means and variances into Equation 4.15, we express the probability of bit error given that symbol '00' was transmitted as

$$\Pr[error \mid s_{00}, \rho, \theta_c] = \frac{1}{2}Q\left(\sqrt{\frac{2E_b}{N_0}} + \sqrt{\frac{2E_j}{N_0}}\cos(\theta_j)\left(\frac{\frac{\rho}{8} - 1}{16}\right)\right) + \frac{1}{2}Q\left(\sqrt{\frac{2E_b}{N_0}} - \sqrt{\frac{2E_j}{N_0}}\sin(\theta_j)\left(\frac{\frac{\rho}{8} - 1}{16}\right)\right) \tag{4.16}$$

where E_b, the signal energy per bit, is

$$E_b = \frac{a_c^2 T_s}{2}$$

and E_j, the jammer energy per bit, is

$$E_j = A_j^2 T_b .$$

It is desirable to eliminate the dependence on the phase angle of the jammer, θ_c, and the number of positive chips in the spreading code, ρ, from the expression for the

probability of bit error given symbol '00' was sent. The dependence on ρ can be removed by considering all possible values of ρ and the probability of error for a given ρ. The probability of bit error is expressed as

$$\Pr\left[error \mid s_{00}, \theta_c\right] = \sum_{\rho=1}^{16} \Pr(\rho) \cdot \Pr\left(error \mid s_{00}, \rho, \theta_c\right). \tag{4.17}$$

The 16-chip LAS spreading codes used by LAS-CDMA have only two possible values of ρ, six and ten. The probabilities of the possible values of ρ for LAS-CDMA are

$$\Pr\left(\rho = 6\right) = \frac{3}{8}$$
$$\Pr\left(\rho = 10\right) = \frac{5}{8}.$$

Substituting the probabilities of ρ into Equation 4.17, we get the probability of bit error given the symbol '00' was transmitted and a jammer phase θ_c is

$$\Pr\left[error \mid s_{00}, \theta_c\right] = \frac{5}{16}\left(Q\left(\sqrt{\frac{2E_b}{N_0}} + \sqrt{\frac{2E_j}{N_0}}\cos(\theta_j)\left(\frac{1}{4}\right)\right) + Q\left(\sqrt{\frac{2E_b}{N_0}} - \sqrt{\frac{2E_j}{N_0}}\sin(\theta_j)\left(\frac{1}{4}\right)\right)\right) +$$
$$\frac{1}{2}\left(Q\left(\sqrt{\frac{2E_b}{N_0}} - \sqrt{\frac{2E_j}{N_0}}\cos(\theta_j)\left(\frac{1}{4}\right)\right) + Q\left(\sqrt{\frac{2E_b}{N_0}} + \sqrt{\frac{2E_j}{N_0}}\sin(\theta_j)\left(\frac{1}{4}\right)\right)\right)$$
. (4.18)

Removing the dependence on θ_c allows this result to be applied to all of the QPSK symbols. The phase angle of the jammer is a uniform random variable between 0 and 2π because the jammer is assumed to have no knowledge of the signal phase. The dependency on the phase angle is eliminated and the probability of bit error becomes

$$P_b = \frac{1}{2\pi}\int_0^{2\pi} \Pr\left[error \mid s_{00}, \theta_c\right] d\theta_c. \tag{4.19}$$

a. Rayleigh Fading

In wireless communications it is necessary to consider the effects of the wireless channel. The wireless channel, in a process known as fading, alters transmitted signals. The wireless channel causes rapid changes in signal strength, frequency modulation due to Doppler shift, and time dispersion due to the multipath channel.

Physical characteristics of the channel influence the effects of fading. Multipath propagation occurs because objects in the channel reflect and scatter the signal, resulting in multiple versions of the signal arriving at the receiver with random amplitude, displaced in time and space. Also, the motion of the mobile station and objects in the channel causes a Doppler shift in the signal. These factors, which combine to cause fading, prevent the strength of signals transmitted in the wireless channel from maintaining a constant value.

Since the strength of signals transmitted through a fading multipath channel cannot be assumed to be a constant, the signal strength must be modeled as a random variable. To perform analysis on the signal performance, assumptions about the channel it is transmitted through need to be made. The channel is assumed to be a flat, slowly fading channel. A flat, slowly fading channel has both a constant gain and a linear phase response over the bandwidth of the transmitted signal and the channel response changes at a much slower rate than the baseband signal. The assumption that the channel is flat and slowly fading is common for analysis of wireless communication systems [7]. For a flat, slowly fading channel without line of sight propagation, it is commonly assumed that the envelope of the received signal can be modeled by a Rayleigh random variable [7]. The Rayleigh probability density function describing the magnitude of the envelope of the received signal is given by [7]

$$f(a_c) = \begin{cases} \dfrac{2a_c}{\overline{a}_c^{\,2}} \exp\left(-\dfrac{a_c^{\,2}}{\overline{a}_c^{\,2}} \right) & 0 \le r < \infty \\ 0 \quad r < 0 \end{cases} \tag{4.20}$$

where $\sqrt{2}a_c$ is the amplitude of the signal and $\overline{a}_c^{\,2}$ is the average power of the received signal. For analysis of a communication system, it is desirable to express the effect of the Rayleigh fading channel as a function of signal-to-noise ratio. The average signal-to-noise ratio is defined as [7]

$$\overline{\gamma} = \frac{2\overline{a}_c^{\,2} T_b}{N_0} \tag{4.21}$$

where T_b is the bit duration, and N_0 is the noise power. A transformation of the random variable is performed to express the effects of the Rayleigh fading channel as a function of

the signal-to-noise ratio. The probability density function for received signal-to-noise ratio in a Rayleigh fading channel is given by [7]

$$f_\gamma(\gamma) = \frac{1}{\overline{\gamma}} e^{\frac{-\gamma}{\overline{\gamma}}} \quad where \quad 0 \le \gamma < \infty . \tag{4.22}$$

Equation 4.18 is viewed as conditional error probability with a fixed signal-to-noise ratio and jammer-to-noise ratio. To obtain bit error probabilities that account for the Rayleigh fading channel we must average $P_b(\gamma,\zeta)$ over the probability density function of γ and ζ, where γ is the signal-to-noise ratio and ζ is the jammer-to-noise ratio. The probability of bit error is found by evaluating the double integral

$$P_b = \int_0^\infty \int_0^\infty P_b(\gamma,\zeta) \frac{1}{\overline{\gamma}} e^{-\frac{\gamma}{\overline{\gamma}}} \frac{1}{\overline{\zeta}} e^{-\frac{\zeta}{\overline{\zeta}}} d\gamma d\zeta . \tag{4.23}$$

Since the jammer is also transmitted through a fading wireless channel, its amplitude can also assumed to be a random variable. Figure 4.4 shows that although the jamming signal also travels through a fading multipath channel, the effects of modeling the jammer as a random variable are small. To simplify the expression for the probability of bit error, the jammer-to-noise ratio is assumed to be non-fading and Equation 4.23 becomes

$$P_b = \int_0^\infty P_b\left(\gamma,\overline{\zeta}\right) \frac{1}{\overline{\gamma}} e^{-\frac{\gamma}{\overline{\gamma}}} d\gamma \tag{4.24}$$

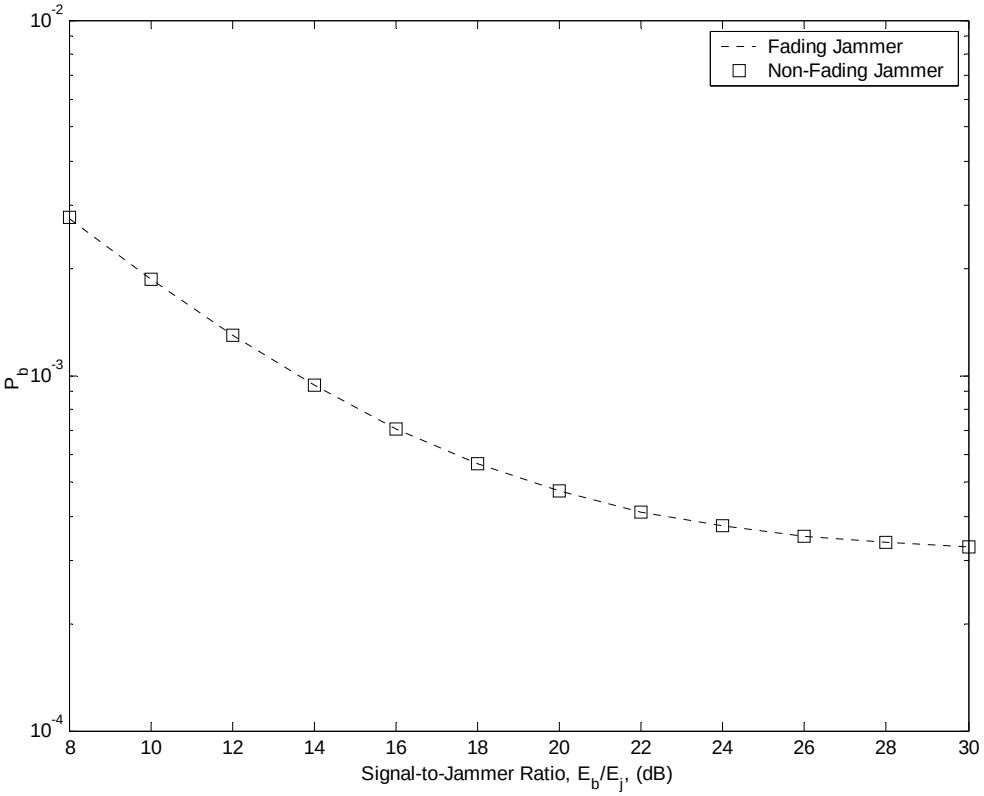

Figure 4.4. Probability of Bit Error for a Fading and Non-Fading Jammer with a Signal-to-Noise Ratio of 29 dB.

The result of the analysis is verified by comparison with the known expression for the probability of bit error without the presence of a tone jammer. The expression for a QPSK signal in AWGN and a Rayleigh fading channel is [14]

$$P_b = \frac{1}{2}\left(1 - \sqrt{\frac{\overline{\gamma}}{1+\overline{\gamma}}}\right). \tag{4.25}$$

Figure 4.5 shows that as the signal-to-jammer ratio increases, the probability of bit error in the presence of a tone jammer asymptotically approaches the probability of bit error in the absence of a tone jammer.

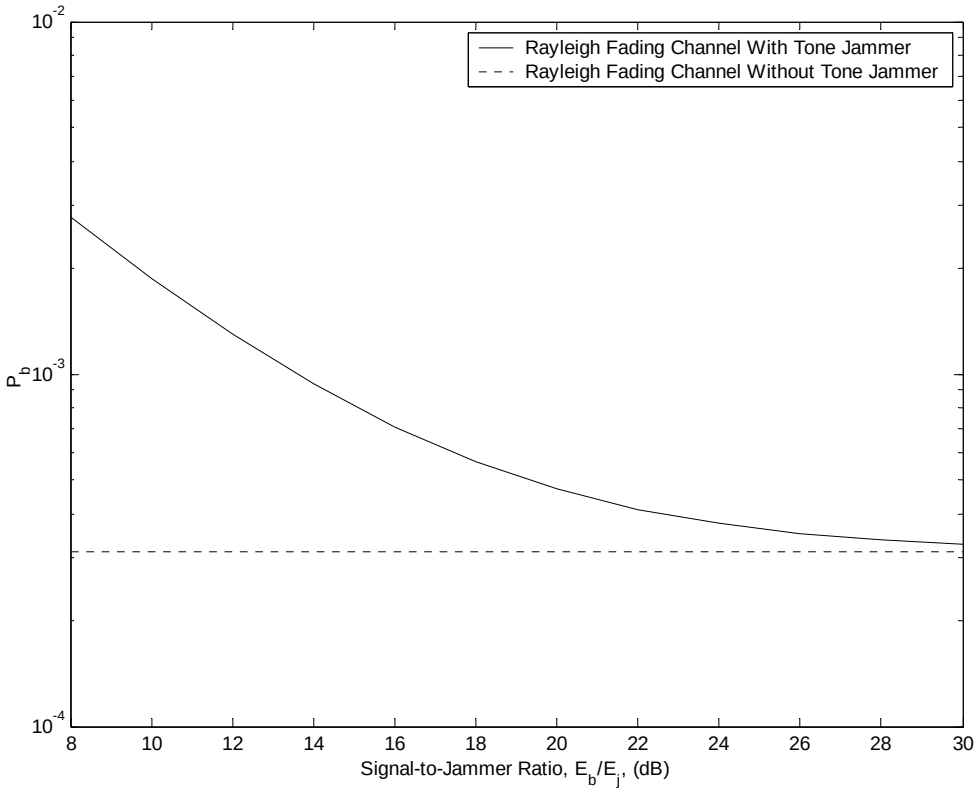

Figure 4.5. Probability of Bit Error in the Presence of a Tone Jammer and in the Absence of a Tone Jammer with a Signal-to-Noise Ratio of 29 dB.

b. Convolutional Coding

The probability of bit error is decreased by the use of convolutional codes. As specified in Chapter II, the Packet Data Channel uses rate 1/2 and rate 3/4, constraint length nine convolutional codes. The probability of bit error is overbounded by [15]

$$P_b < \frac{1}{k} \sum_{d=d_{free}}^{\infty} B_d P_d \tag{4.26}$$

where k is the number of data bits that generate n coded bits, B_d represents the sum of all possible bit errors that can on all weight d paths occur and is dependent on the code that is used, and P_d is the probability of selecting a code sequence that is a Hamming distance d from the correct code sequence. P_d is dependent on the channel probability of bit error and whether hard decision or soft decision decoding is used. This thesis assumes hard

decision decoding. Greater coding gains are capable with soft decision decoding, but the complexity of the decoder and analysis also increases.

Although P_d and B_d are summed from d_{free} to infinity, the summation is generally reduced to only the first few non-zero values of B_d. The first four non-zero values of B_d for the rate 1/2, constraint length nine convolution code are listed in Table 4.1. Table 4.2 lists the first four non-zero values of B_d for the optimal punctured rate ¾ convolutional code with eight memory elements. LAS-CDMA does not use the punctured code, but the optimal punctured code is a close upperbound for the convolutional code with the same rate and number of memory elements.

Table 4.2. Rate 1/2, Constraint Length Nine, Convolutional Code Information Weight Structure. After Ref [15].

d_{free}	B_{dfree}	$B_{dfree+1}$	$B_{dfree+2}$	$B_{dfree+3}$	$B_{dfree+4}$	$B_{dfree+5}$	$B_{dfree+6}$
12	33	0	281	0	2179	0	15035

Table 4.3. Punctured Rate 3/4 Convolutional Code Information Weight Structure. After Ref [15].

d_{free}	B_{dfree}	$B_{dfree+1}$	$B_{dfree+2}$	$B_{dfree+3}$	$B_{dfree+4}$
6	12	342	1996	12296	78145

A decoding error occurs when the received code word agrees with an incorrect code word in $d/2$ or more positions. For hard decision decoding, the probability of selecting a code word that is a Hamming distance d from the correct code word when d is odd is [15]

$$P_d = \sum_{i=\frac{d+1}{2}}^{d} \binom{d}{i} p^i (1-p)^{d-i} \tag{4.27}$$

where p is the probability of channel bit error calculated in Equation 4.24. When d is even there is the possibility of the event of a tie between the correct and incorrect path. In the

case of a tie there is a fifty percent chance of making an error. The probability of selecting an incorrect path when d is even is [15]

$$P_d = \frac{1}{2}\binom{d}{d/2} p^{d/2}(1-p)^{d/2} + \sum_{i=\frac{d}{2}+1}^{d} \binom{d}{i} p^i (1-p)^{d-i} \tag{4.28}$$

The expressions for P_d from Equation 4.27 and Equation 4.28 and the values of B_d from Table 4.2 and Table 4.3 are combined according to Equation 4.26. The resulting probabilities of error for MCS 1 and MCS 2 of the Packet Data Channel are displayed in Figure 4.5 and Figure 4.6.

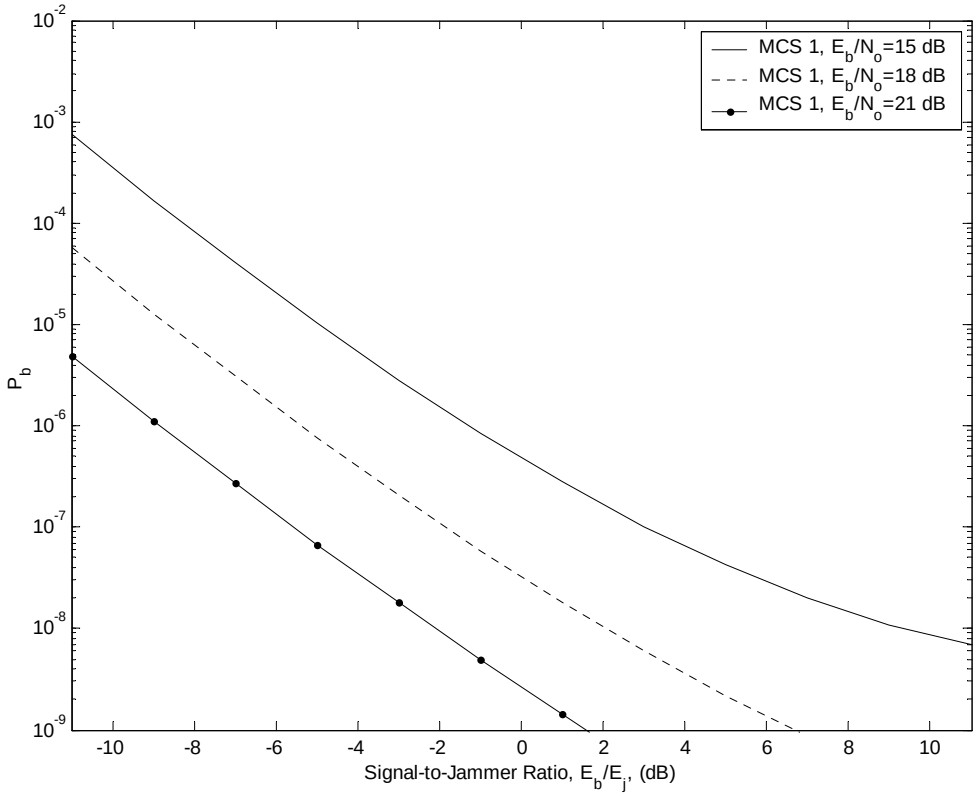

Figure 4.5. Probability of Bit Error vs. Signal to Jammer Ratio for Packet Data Channel, MCS 1.

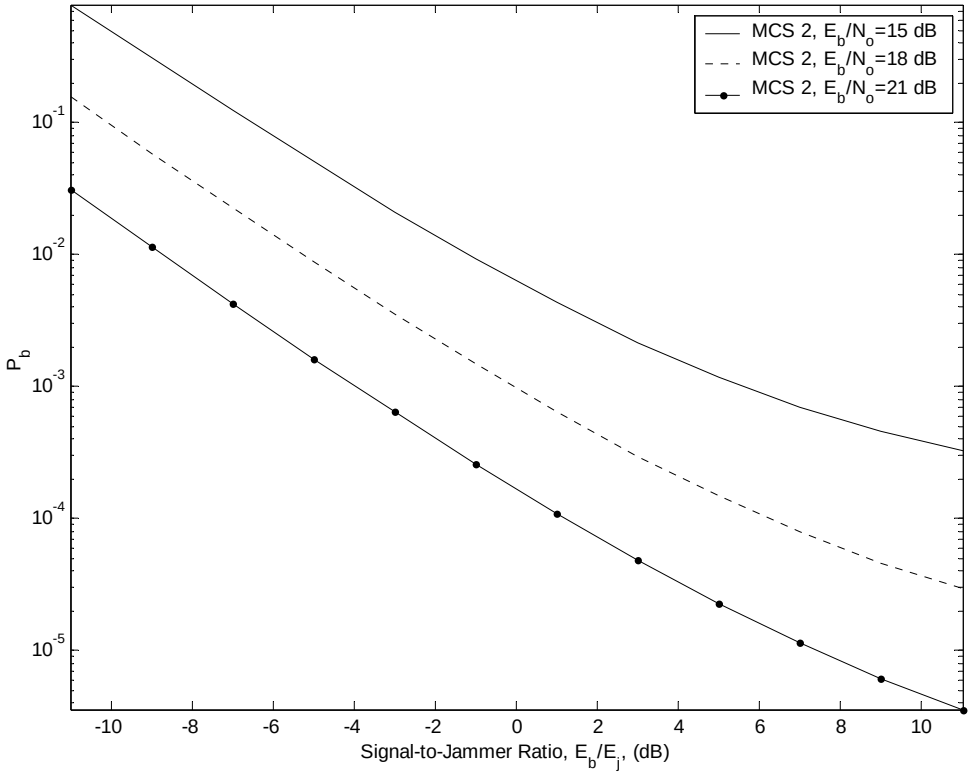

Figure 4.6. Probability of Bit Error vs. Signal to Jammer Ratio for Packet Data Channel, MCS 2.

2. 8-PSK

LAS-CDMA transmits an 8-PSK signal on the Packet Data Channel using the signal constellation illustrated in Figure 4.7. The 8-PSK, spread spectrum signal is represented by [14]

$$s_{m,i}(t) = \sqrt{2}a_c c(t)\cos\left(w_c t + \frac{2\pi i + \pi}{8}\right) \quad \begin{matrix} 0 \le t \le T_s \\ i = 1,..,8 \end{matrix}. \tag{4.29}$$

The QPSK demodulator illustrated in Figure 4.3 is also used to receive 8-PSK.

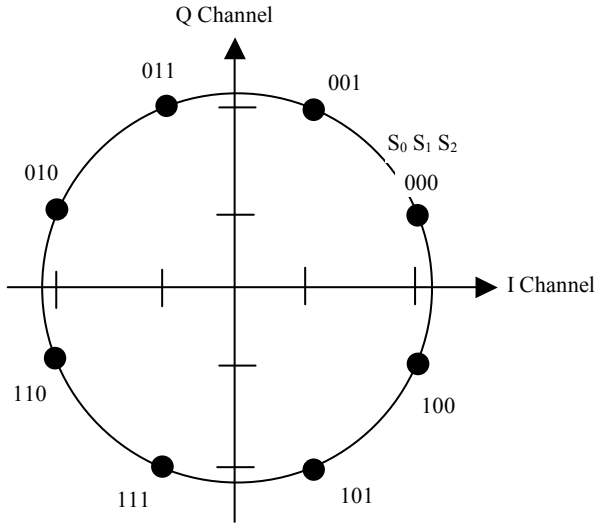

Figure 4.7. 8-PSK Signal Constellation. After Ref [9].

The 8-PSK signal received in the presence of AWGN and a tone jammer is expressed as

$$r(t) = \sqrt{2}a_c c(t)\left[\cos\theta_m \cos w_c t - \sin\theta_m \sin w_c t\right] + \sqrt{2}a_j\left[\cos\theta_j \cos w_c t - \sin\theta_j \sin w_c t\right] + n(t) \tag{4.30}$$

where the message phase angle is

$$\theta_m = \frac{2\pi i + \pi}{8}.$$

Similar to QPSK, it can be shown that at the integrator outputs the in-phase and quadrature branches of the 8-PSK receiver are independent and can be modeled as Gaussian random variables. The received signal is demodulated by in-phase and quadrature correlation receivers. The expected value at the output of the in-phase correlator is

$$\overline{X} = \sqrt{2}a_T \cos\theta_T \tag{4.31}$$

and the expected value of the output of the quadrature correlator is

$$\overline{Y} = \sqrt{2}a_T \sin\theta_T \tag{4.32}$$

where

$$a_T = \sqrt{a_c^2 + \frac{2a_c a_j\left(\frac{\rho}{8}-1\right)\cos(\theta_j+\theta_m)}{16} + \frac{a_j^2\left(\frac{\rho}{8}-1\right)^2}{16^2}} \tag{4.33}$$

and

$$\theta_T = \tan^{-1}\left(\frac{a_c\sin\theta_m + \frac{a_j\left(\frac{\rho}{8}-1\right)\sin\theta_j}{16}}{a_c\cos\theta_m + \frac{a_j\left(\frac{\rho}{8}-1\right)\cos\theta_j}{16}}\right). \tag{4.34}$$

The vector representation of a_T and θ_T is illustrated in Figure 4.8. Analogous to QPSK, the noise power of the in-phase and quadrature components is the variance of the Gaussian random variables.

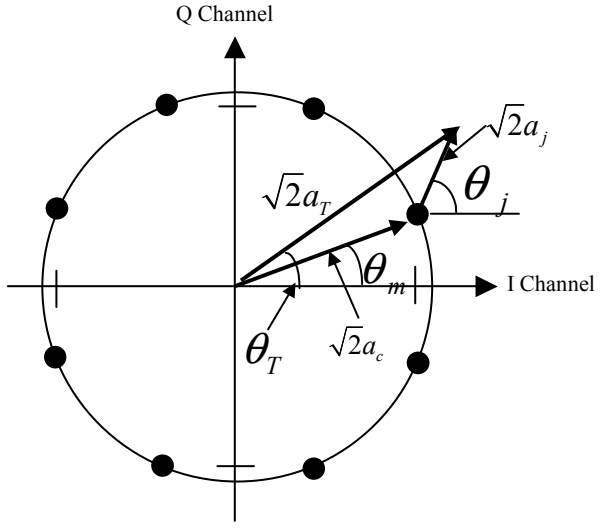

Figure 4.8. Vector Representation of a_T and θ_T.

The outputs of the in-phase and quadrature correlators are modeled as Gaussian random variables as in the QPSK case. The probability density functions for the in-phase and quadrature correlator outputs conditioned on the phase angle transmitted are

$$f_X(x \mid \theta_m) = \frac{1}{\sqrt{2\pi}\sigma} e^{\frac{-\left(x-\sqrt{2}a_T \cos(\theta_T)\right)^2}{2\sigma^2}} \tag{4.35}$$

$$f_Y(y \mid \theta_m) = \frac{1}{\sqrt{2\pi}\sigma} e^{\frac{-\left(y-\sqrt{2}a_T \sin(\theta_T)\right)^2}{2\sigma^2}} . \tag{4.36}$$

The data, transmitted in the phase of received signal, is recovered by taking the inverse tangent of the division the output of the in-phase correlator by the output of the quadrature correlator. In order to calculate the probability of symbol error for a given jammer phase, all the possible transmitted message phases need to be considered. Allowing the phase of the jammer to be a uniform random variable on the range from 0 to 2π ensures that the probability of symbol error for all the possible message phases is equal. Since the probability of symbol error for all possibilities are equal, only one case needs to be considered. The transmitted phase is assumed to be $\pi/8$. The phase angle of the received signal given the transmitted signal had a phase of $\pi/8$ is

$$f_{\hat{\theta}}\left(\hat{\theta} \mid \theta_T(\pi/8)\right) = \frac{e^{-\frac{a_T{}^2 T_s}{N_0}}}{2\pi} + \sqrt{\frac{a_T^2 T_s}{\pi N_0}} e^{-\frac{a_T^2 T_s \sin^2\left(\hat{\theta}-\theta_T(\pi/8)\right)}{N_0}} \cos\left(\hat{\theta}-\theta_T(\pi/8)\right) \times\left\{1-Q\left(\sqrt{\frac{a_T^2 T_s}{\pi N_0}}\cos\left(\hat{\theta}-\theta_T(\pi/8)\right)\right)\right\} . \tag{4.37}$$

For 8PSK, assuming the transmitted phase angle is $\pi/8$, the upper bound is $\pi/4$ and the lower bound is 0. An error occurs when the phase angle of the received signal does not fall within these bounds. The probability of symbol error for an 8PSK LAS-CDMA signal in the presence of a tone jammer is

$$P_s = 1 - \int_0^{\pi/4} f_{\hat{\theta}}(\hat{\theta} \mid \theta_T(\pi/8)) d\hat{\theta} . \tag{4.38}$$

With simplification, Equation 4.38 becomes

$$P_s = \frac{1}{8} e^{-\frac{a_T^2 T_s}{N_0}} + Q\left(\sqrt{\frac{2a_T^2 T_s}{N_0}} \sin\left(\frac{\pi}{4} - \theta_T\right)\right) + Q\left(\sqrt{\frac{2a_T^2 T_s}{N_0}} \sin\left(\theta_T\right)\right)$$
$$+ \sqrt{\frac{a_T^2 T_s}{\pi N_0}} \int_0^{\pi/4} e^{-\frac{a_T^2 T_s \sin^2\left(\hat{\theta} - \theta_T(\pi/8)\right)}{N_0}} \cos\left(\hat{\theta} - \theta_T(\pi/8)\right) Q\left(\sqrt{\frac{a_T^2 T_s}{\pi N_0}} \cos\left(\hat{\theta} - \theta_T(\pi/8)\right)\right) d\theta \quad (4.39)$$

This integral must be evaluated numerically, but when

$$\sqrt{\frac{a_T^2 T_s}{\pi N_0}} \cos\left(\hat{\theta} - \theta_T(\pi/8)\right) >> 1$$

we can make the approximation

$$Q\left(\sqrt{\frac{a_T^2 T_s}{\pi N_0}} \cos\left(\hat{\theta} - \theta_T(\pi/8)\right)\right) \approx \frac{1}{2\sqrt{\pi a_T^2 T / N_0} \cos\left(\hat{\theta} - \theta_T(\pi/8)\right)} e^{-\left(\frac{a_T^2 T}{N_0} \cos^2\left(\hat{\theta} - \theta_T(\pi/8)\right)\right)}. \quad (4.40)$$

Substituting in the approximation for the Q function, the probability of symbol error becomes

$$P_s = Q\left(\sqrt{\frac{2a_T^2 T_s}{N_0}} \sin\left(\frac{\pi}{4} - \theta_T\right)\right) + Q\left(\sqrt{\frac{2a_T^2 T_s}{N_0}} \sin\left(\theta_T\right)\right). \quad (4.41)$$

An approximation for probability of bit error follows from the probability of symbol error by assuming that all symbol errors are detected as adjacent symbols. Gray coding ensures that adjacent symbols differ only by one bit. For M-ary modulation each symbol contains *m* bits where $M = 2^m$. The probability of bit error for M-ary modulation is approximated as [14]

$$P_b \approx \frac{1}{m} P_s. \quad (4.42)$$

Using the approximation for the probability of bit error in Equation 4.42, the probability of bit error for 8PSK becomes

$$P_b = \frac{1}{3} Q\left(\sqrt{\frac{2a_T^2 T_s}{N_0}} \sin\left(\frac{\pi}{4} - \theta_T\right)\right) + \frac{1}{3} Q\left(\sqrt{\frac{2a_T^2 T_s}{N_0}} \sin\left(\theta_T\right)\right). \quad (4.43)$$

This result is applied to LAS-CDMA by substituting in for the appropriate values and probabilities of ρ. Equation 4.43 becomes

$$P_s(\rho)=\frac{5}{24}Q\left(\sqrt{2\left[E_b+\frac{\sqrt{E_bE_j}}{2}+\frac{E_j}{16}\right]}\sin\left(\frac{\pi}{4}-\theta_T(10)\right)\right)+\frac{5}{24}Q\left(\sqrt{2\left[E_b+\frac{\sqrt{E_bE_j}}{2}+\frac{E_j}{16}\right]}\sin\left(\theta_T(10)\right)\right)$$
$$+\frac{1}{8}Q\left(\sqrt{2\left[E_b-\frac{\sqrt{E_bE_j}}{2}+\frac{E_j}{16}\right]}\sin\left(\frac{\pi}{4}-\theta_T(6)\right)\right)+\frac{1}{8}Q\left(\sqrt{2\left[E_b-\frac{\sqrt{E_bE_j}}{2}+\frac{E_j}{16}\right]}\sin\left(\theta_T(6)\right)\right) \tag{4.44}$$

where the transmitted energy per bit is

$$E_b=\frac{a_c^2T_s}{3},$$

the transmitted jammer energy is

$$E_j=a_j^2T_s,$$

and

$$\theta_T(\rho)=\tan^{-1}\left(\frac{\sqrt{E_b}\sin\frac{\pi}{8}+\sqrt{E_j}\left(\frac{\rho}{8}-1\right)\sin\theta_j}{\sqrt{E_b}\cos\frac{\pi}{8}+\sqrt{E_j}\left(\frac{\rho}{8}-1\right)\cos\theta_j}\right). \tag{4.45}$$

The effects of the Rayleigh fading channel and error correction coding on the probability of bit error from Equation 4.44 are considered. The resulting probability of bit error for an 8PSK signal in the presence of a tone jammer in a Rayleigh fading channel with rate 1/2 convolutional coding is displayed in Figure 4.9. Figure 4.10 displays the probability of bit error for an 8PSK signal in the presence of a tone jammer in a Rayleigh fading channel with rate 3/4 convolutional coding.

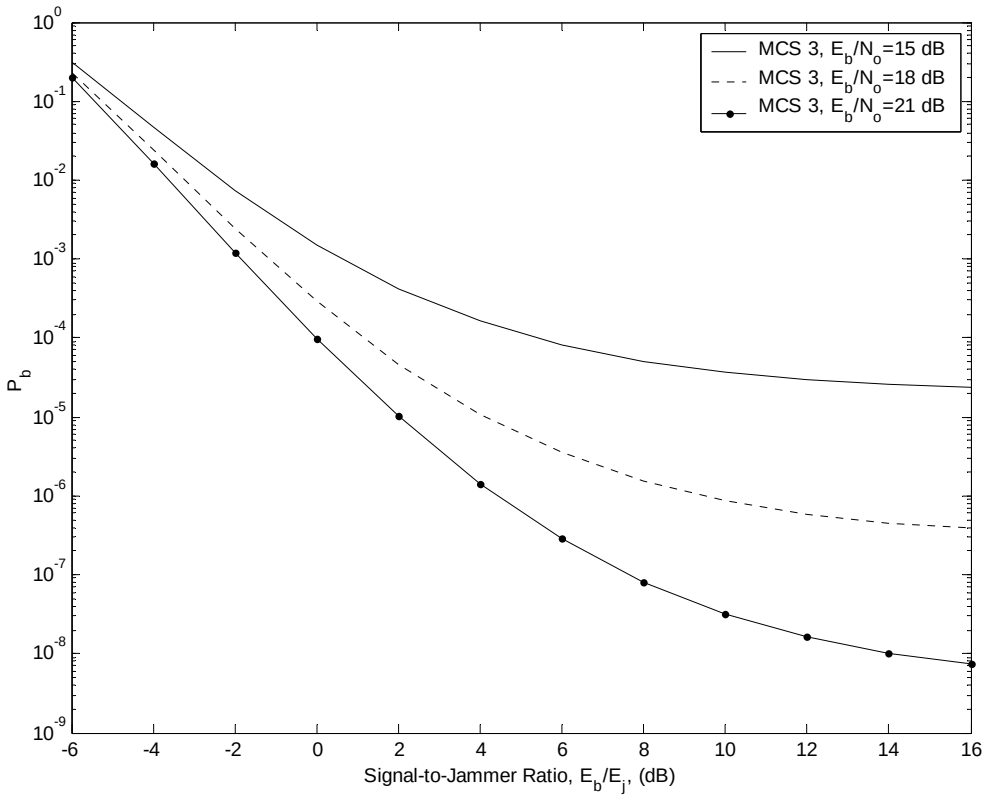

Figure 4.9. Probability of Bit Error vs. Signal to Jammer Ratio for Packet Data Channel, MCS 3.

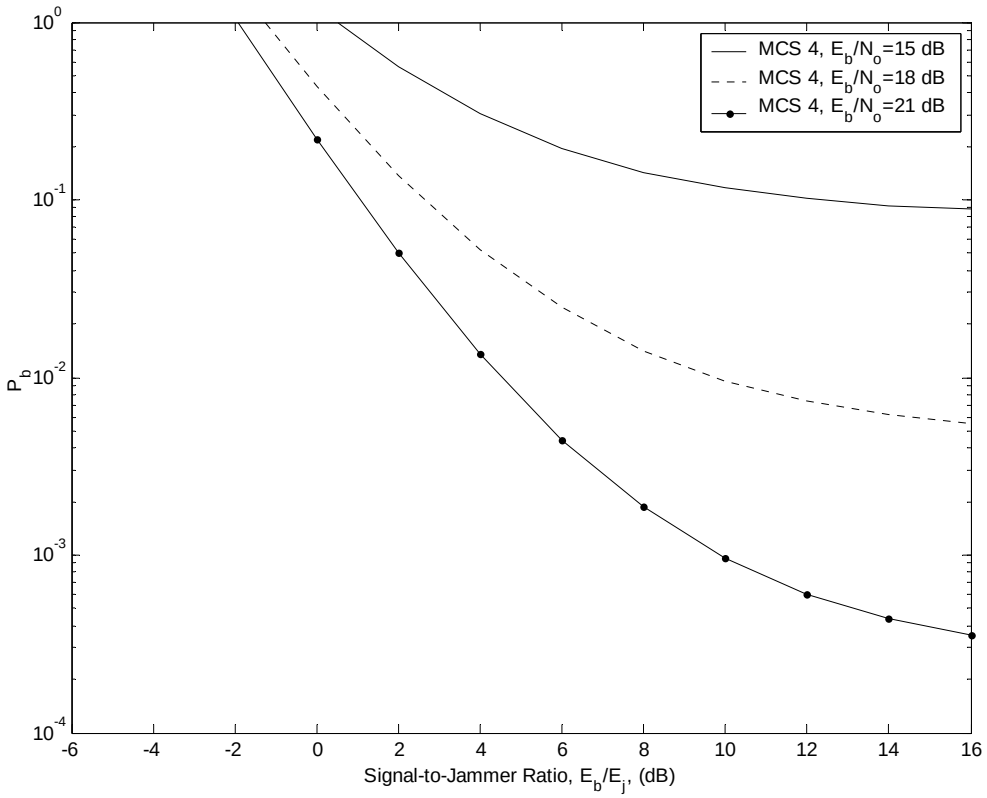

Figure 4.10. Probability of Bit Error vs. Signal to Jammer Ratio for Packet Data Channel, MCS 4.

3. Quadrature Amplitude Modulation

The Packet Data Channel uses quadrature amplitude modulation (QAM) to maintain a constant symbol rate and achieve higher data rates than QPSK and 8PSK. 16-QAM and 64-QAM are used to modulate the Packet Data Channel. A general analysis of the probability of bit error for M-QAM where $M = 2^m$ and m is even is preformed. The analysis is applied to both 16-QAM and 64-QAM. The analysis can be applied to both 16-QAM and 64-QAM because both are modulated using square constellations. The signal constellation for 16-QAM is illustrated in Figure 4.11. Figure 4.12 illustrates the signal constellation for 32-QAM.

The received M-QAM, spread spectrum waveform is expressed by [14]

$$r(t) = \sqrt{2}a_I(t)c(t)\cos(w_c t) + \sqrt{2}a_Q(t)c(t)\sin(w_c t) + \sqrt{2}a_j\cos\left(w_c t + \theta_c\right) + n(t) \quad (4.46)$$

where $\sqrt{2}a_I$ is the amplitude of the in-phase signal component and $\sqrt{2}a_Q$ is the amplitude of the quadrature signal component. The M-QAM, spread spectrum signal can be separated into two $\sqrt{M}$ -PAM, spread spectrum signals because *m* is even. The received in-phase $\sqrt{M}$ -PAM, spread spectrum waveform is expressed as [14]

$$r_I(t) = \sqrt{2}a_I c(t)\cos(w_c t) + \sqrt{2}a_j \cos(\theta_c)\cos(w_c t) + n_I(t) \tag{4.47}$$

where

$$a_I = \sqrt{2}a_o\left(2l - 1 - \sqrt{M}\right) \quad for \quad l = 1, 2, ..., \sqrt{M} \tag{4.48}$$

and $n_I(t)$ is the in-phase component of the noise.

.

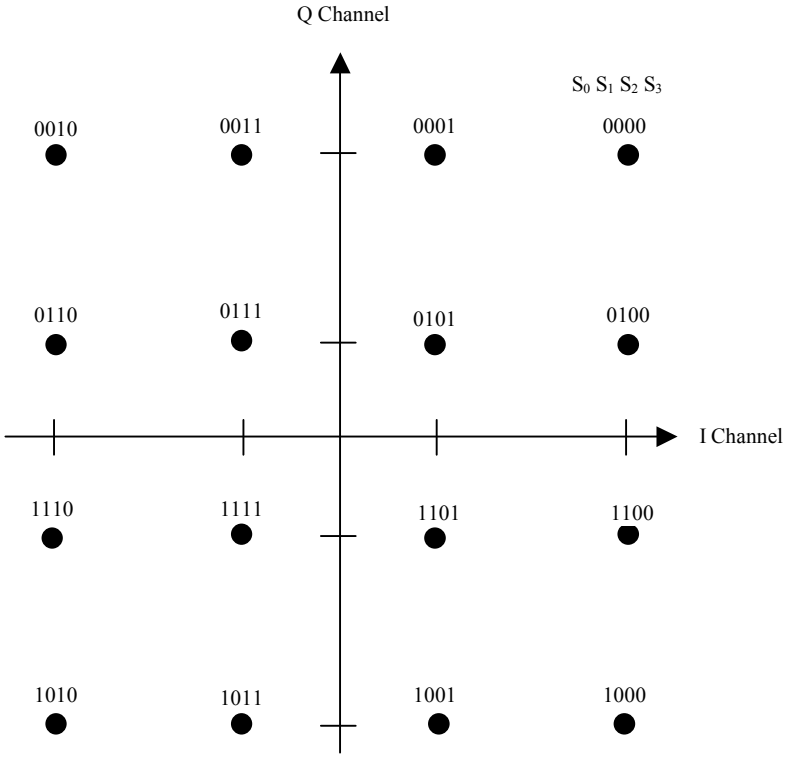

Figure 4.11. 16-QAM Signal Constellation. After Ref [9].

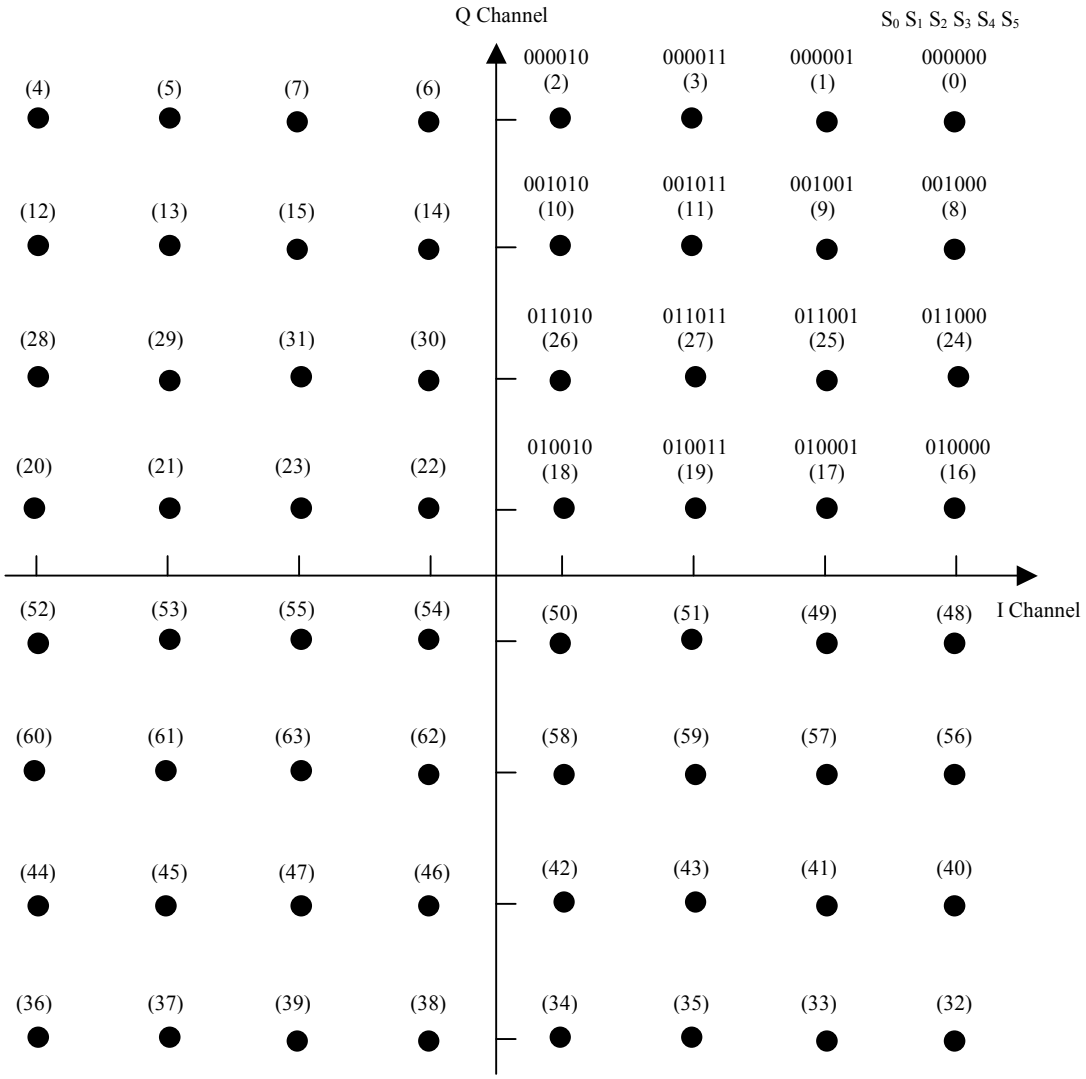

Figure 4.12. 64-QAM Signal Constellation. After Ref [9].

The $\sqrt{M}$ -PAM signal is demodulated using maximum likelihood detection. The M-QAM demodulator uses two $\sqrt{M}$ -PAM demodulators to detect the signal. The M-QAM demodulator is illustrated in Figure 4.13. Coherent PAM detection in the presence of AWGN is similar to the QPSK case considered previously. The in-phase and quadrature correlators produce outputs that are modeled as Gaussian random variables. The expected value of the output of the in-phase correlator is

$$\bar{X} = a_I + a_j \cos(\theta_c)\left(\frac{\rho}{8} - 1\right) \tag{4.49}$$

and the variance is

$$\sigma_X^2 = \frac{N_o}{T_s}.$$

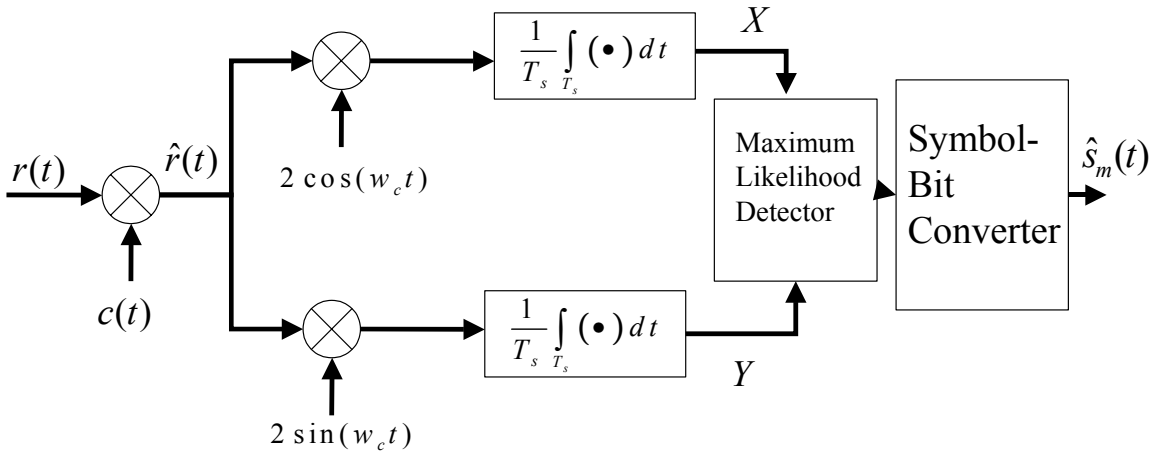

Figure 4.13. M-QAM Demodulator. After Ref [14].

To determine the probability of symbol error for an in-phase PAM bit, four cases need to be considered, when a_I is minimum, a_I is maximum, a_I is negative, but not minimum, and a_I is positive, but not maximum. It is assumed that all values of a_I are equally likely and the decision thresholds are set so there is a uniform distance between signal values and the threshold. The probability of symbol error in the presence of a tone jammer given the value of a_I transmitted is positive, but not the maximum, is

$$P_{s(\text{int})^+}(\rho) = 1 - \frac{1}{\sqrt{2\pi}\sigma}\int_0^{2\sqrt{2}a_o} e^{-\frac{(x-\sqrt{2}a_o - a_j\cos(\theta)(\rho/8-1))^2}{2\sigma^2}}\,dx. \tag{4.50}$$

In terms of the Q-function Equation 4.50 becomes

$$P_{s(\text{int})^+}(\rho) = Q\left(\sqrt{\frac{2a_o^2}{\sigma^2}}\left(1+\sqrt{\frac{a_j^2}{a_o^2}}\cos(\theta)\left(\frac{\rho}{8}-1\right)\right)\right) + Q\left(\sqrt{\frac{2a_o^2}{\sigma^2}}\left(1-\sqrt{\frac{a_j^2}{a_o^2}}\cos(\theta)\left(\frac{\rho}{8}-1\right)\right)\right) \tag{4.51}$$

It can be shown that the probability of symbol error given the value of A_I transmitted is negative, but not the minimum, is equal to the probability of symbol error given the value of A_I transmitted is positive, but not the maximum. Therefore, the probability of symbol error given the value of A_I transmitted is negative, but not the minimum, is

$$P_{s(\text{int})^-}(\rho) = P_{s(\text{int})^+}(\rho) = Q\left(\sqrt{\frac{2a_o^2}{\sigma^2}}\left(1+\sqrt{\frac{a_j^2}{a_o^2}}\cos(\theta)\left(\frac{\rho}{8}-1\right)\right)\right) + Q\left(\sqrt{\frac{2a_o^2}{\sigma^2}}\left(1-\sqrt{\frac{a_j^2}{a_o^2}}\cos(\theta)\left(\frac{\rho}{8}-1\right)\right)\right). \quad (4.52)$$

Similarly the probability of symbol error when a_I is maximum and when a_I is minimum can be calculated. When the value of a_I transmitted is maximum, the probability of error is

$$P_{s(\max)}(\rho) = 1-\frac{1}{\sqrt{2\pi}\sigma}\int_0^\infty e^{-\frac{(x-\sqrt{2}a_o-a_j\cos(\theta)(\rho/8-1))^2}{2\sigma^2}}dx = Q\left(\sqrt{\frac{2a_o^2}{\sigma^2}}\left(1+\sqrt{\frac{a_j^2}{a_o^2}}\cos(\theta)\left(\frac{\rho}{8}-1\right)\right)\right). \quad (4.53)$$

The probability of symbol when A_I transmitted is minimum is

$$P_{s(\min)}(\rho) = \frac{1}{\sqrt{2\pi}\sigma}\int_0^\infty e^{-\frac{(x+\sqrt{2}a_o-a_j\cos(\theta)(\rho/8-1))^2}{2\sigma^2}}dx = Q\left(\sqrt{\frac{2a_o^2}{\sigma^2}}\left(1-\sqrt{\frac{a_j^2}{a_o^2}}\cos(\theta)\left(\frac{\rho}{8}-1\right)\right)\right). \quad (4.54)$$

Using the concept of total probability, the probability of error is the summation of each case multiplied the probability of error for that case. Applying the concept of total probability to the probability of error for an in-phase $\sqrt{M}$ -PAM waveform yields

$$P_{s_I}(\rho) = \frac{1}{\sqrt{M}}\left[\left(\frac{\sqrt{M}}{2}-1\right)P_{b(\text{int})^+}(\rho)+\left(\frac{\sqrt{M}}{2}-1\right)P_{b(\text{int})^-}(\rho)+P_{b(\max)}(\rho)+P_{b(\min)}(\rho)\right] \quad .(4.55)$$

Substituting the into Equation 4.55, we get the probability of symbol error for the in-phase $\sqrt{M}$ -PAM waveform is

$$P_{s_I}(\rho)=\left(1-\frac{1}{\sqrt{M}}\right)Q\left(\sqrt{\frac{3E_s}{N_o(M-1)}}+\sqrt{2\frac{E_j}{N_o}}\cos(\theta)\left(\frac{\rho}{8}-1\right)\right)$$
$$+\left(1-\frac{1}{\sqrt{M}}\right)Q\left(\sqrt{\frac{3E_s}{N_o(M-1)}}-\sqrt{2\frac{E_j}{N_o}}\cos(\theta)\left(\frac{\rho}{8}-1\right)\right) \quad (4.56)$$

where E_s, the average energy per symbol, is

$$E_s=\frac{2a_o^2}{3}(M-1).$$

The ρ dependence can be eliminated from the probability of error of the in-phase PAM waveform by multiplying by the probability of ρ positive chips occurring in the spreading code and summing over all valid ρ. Using the valid values and probabilities of ρ for LAS-CDMA the probability of symbol error for the in-phase $\sqrt{M}$ -PAM waveform is

$$P_{s_I}(\rho)=\left(1-\frac{1}{\sqrt{M}}\right)Q\left(\sqrt{\frac{3E_s}{N_o(M-1)}}+\sqrt{2\frac{E_j}{N_o}}\cos(\theta)\frac{1}{4}\right)$$
$$+\left(1-\frac{1}{\sqrt{M}}\right)Q\left(\sqrt{\frac{3E_s}{N_o(M-1)}}-\sqrt{2\frac{E_j}{N_o}}\cos(\theta)\frac{1}{4}\right). \quad (4.57)$$

Through analogous calculations it can be shown that the probability of symbol error for the quadrature $\sqrt{M}$ -PAM waveform is

$$P_{s_Q}(\rho)=\left(1-\frac{1}{\sqrt{M}}\right)Q\left(\sqrt{\frac{3E_s}{N_o(M-1)}}+\sqrt{2\frac{E_j}{N_o}}\sin(\theta)\frac{1}{4}\right)$$
$$+\left(1-\frac{1}{\sqrt{M}}\right)Q\left(\sqrt{\frac{3E_s}{N_o(M-1)}}-\sqrt{2\frac{E_j}{N_o}}\sin(\theta)\frac{1}{4}\right). \quad (4.58)$$

The in-phase and quadrature $\sqrt{M}$ -PAM waveforms can be assumed to be independent; therefore, the probabilities of symbol error for the in-phase and quadrature $\sqrt{M}$ -PAM waveforms are independent. The probability of bit error can be related to the probability of symbol error by using the approximation in Equation 4.42. The probability of bit error for a M-QAM, spread spectrum signal expressed as a function of the $\sqrt{M}$ -PAM in-phase and quadrature components is

$$P_b \approx \frac{1}{\log_2 M}\left(P_{s_I} + P_{s_Q} - P_{s_I} \bullet P_{s_Q}\right) \tag{4.59}$$

The Rayleigh fading channel and convolutional encoding affects the probability of bit error for the M-QAM signal in an analogous fashion as the QPSK and 8PSK signals. The probability of bit error for a 16-QAM, spread spectrum signal with rate 1/2 convolutional coding in the presence of a tone jammer is plotted in Figure 4.14. Figure 4.15 illustrates the probability of bit error for a 16-QAM, spread spectrum signal with rate 3/4 convolutional coding in the presence of a tone jammer. The probability of bit error for a 64-QAM, spread spectrum signal with rate 1/2 convolutional coding in the presence of a tone jammer is plotted in Figure 4.16, and the probability of bit error for a 64-QAM, spread spectrum signal with rate 3/4 convolutional coding in the presence of a tone jammer is plotted in Figure 4.17

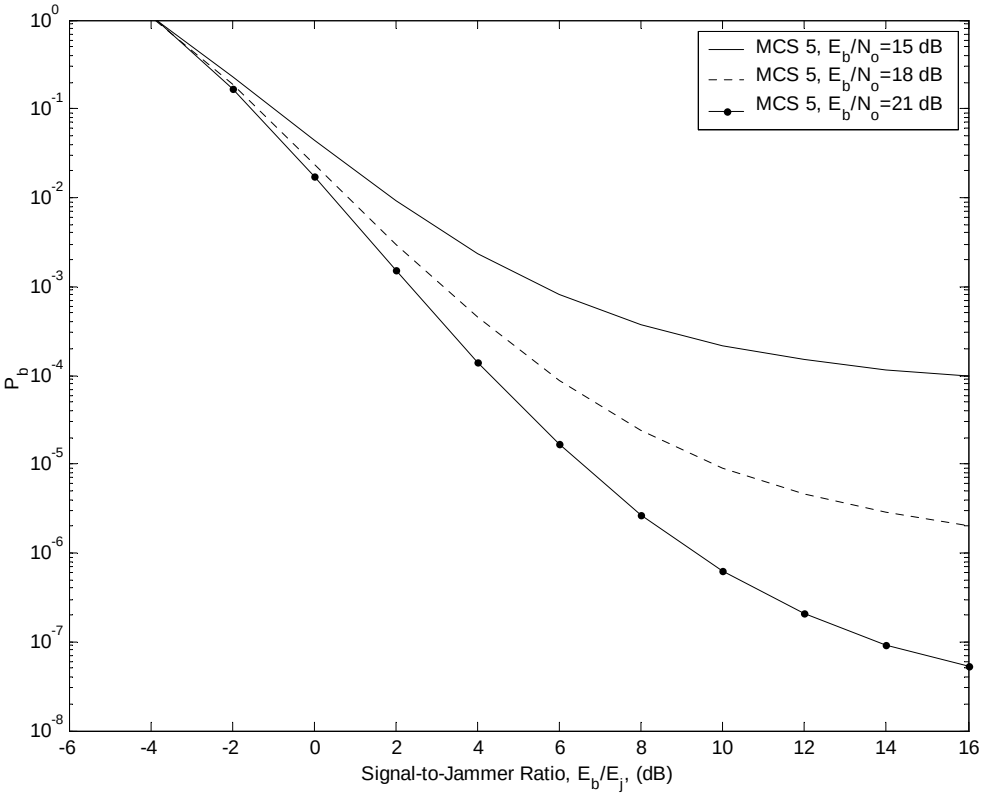

Figure 4.14. Probability of Bit Error vs. Signal to Jammer Ratio for Packet Data Channel, MCS 5.

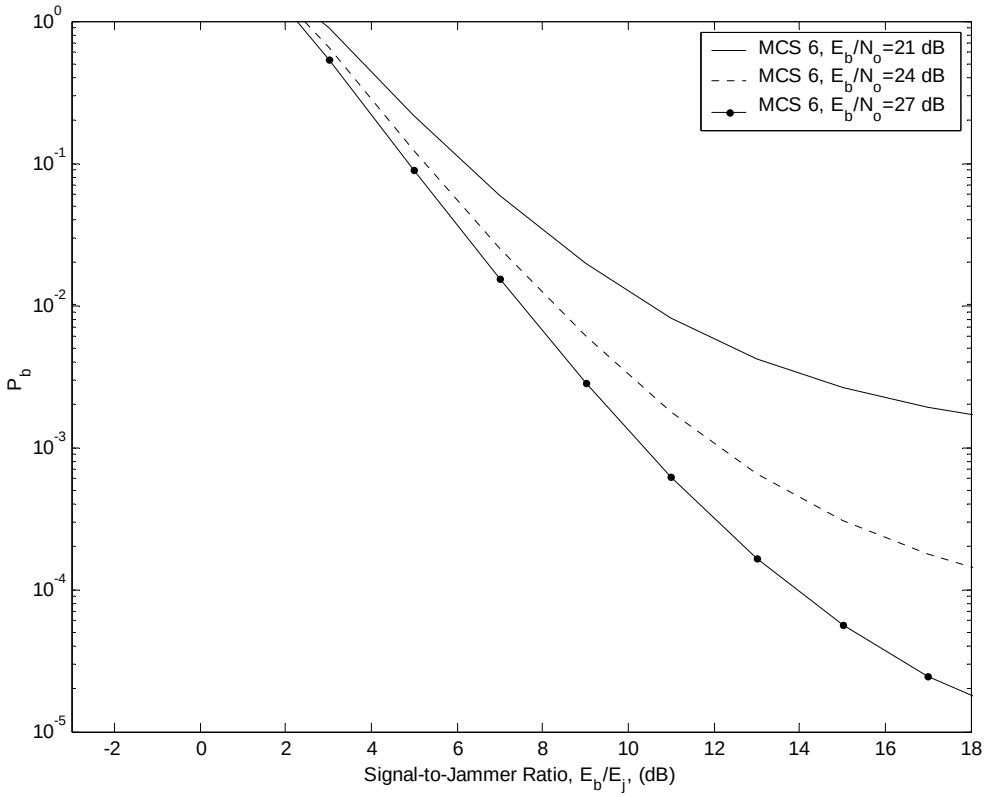

Figure 4.15. Probability of Bit Error vs. Signal to Jammer Ratio for Packet Data Channel, MCS 6.

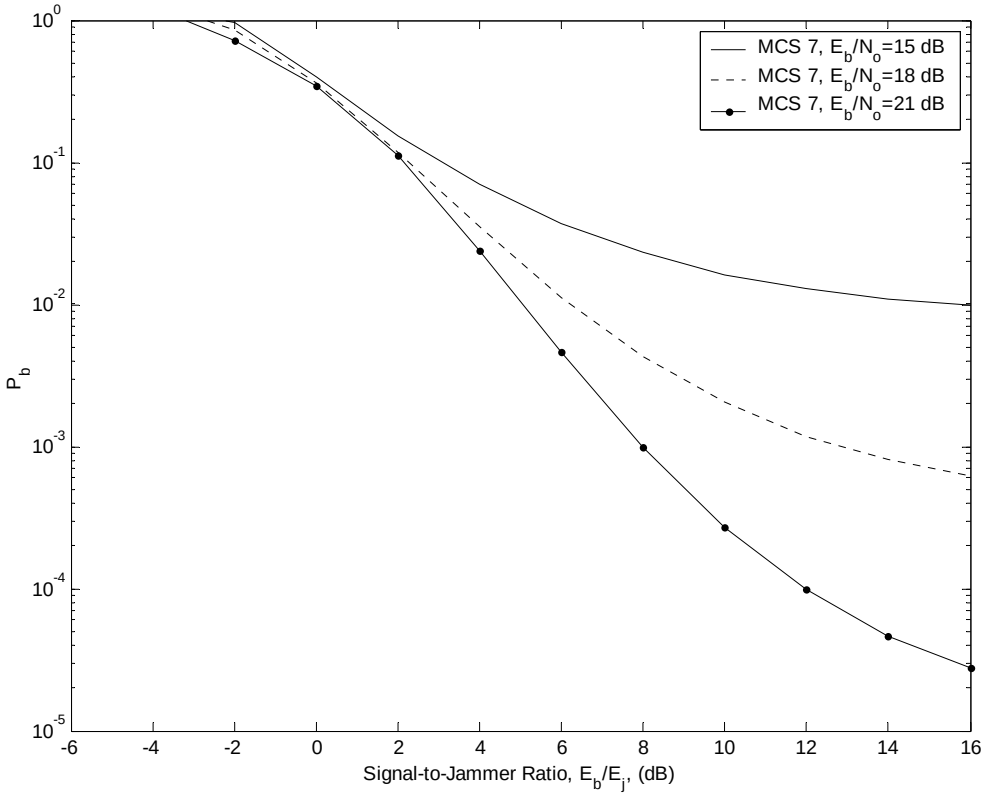

Figure 4.16. Probability of Bit Error vs. Signal to Jammer Ratio for Packet Data Channel, MCS 7.

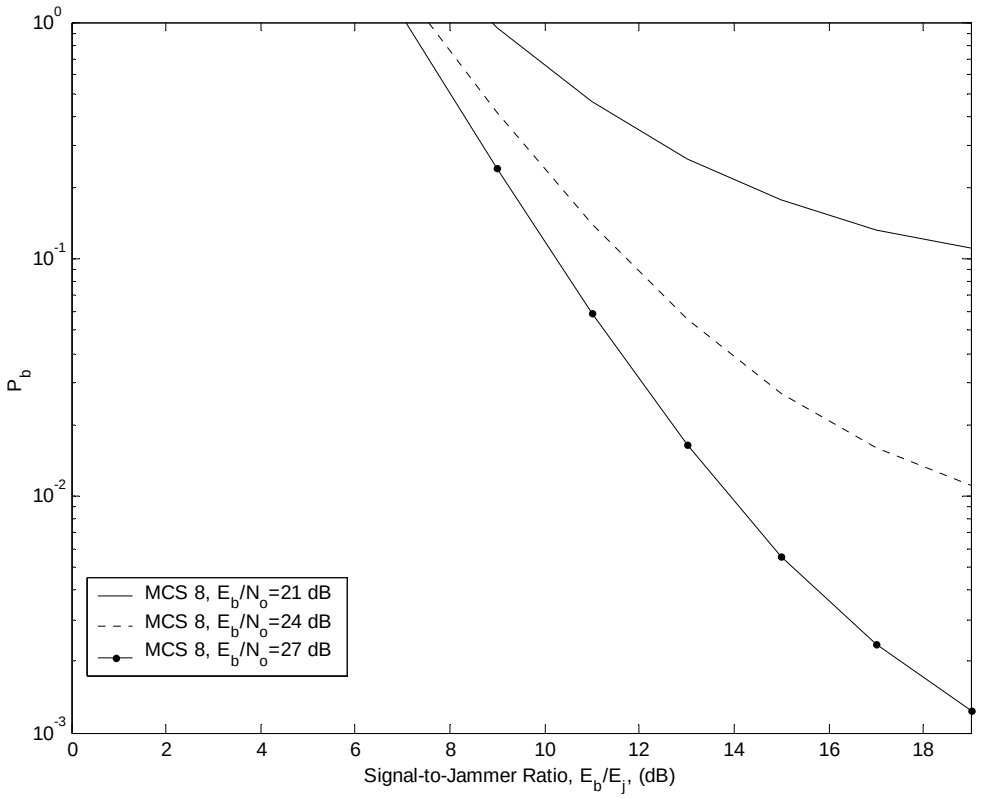

Figure 4.17. Probability of Bit Error vs. Signal to Jammer Ratio for Packet Data Channel, MCS 6

4. Performance Comparison of Modulation and Coding Schemes

The performance of the modulation and coding schemes used in the Packet Data Channel are compared. For a signal-to-noise ratio of 21 dB, the probability of bit error for the different modulation and coding schemes are plotted in Figure 4.18. We would expect that LAS-CDMA would be designed such that the probability of bit error increases as the data rate increases. This is not the case. Dividing the data in two subsets according to convolutional code rate, we notice that within each subset that the probability of bit error does increase as the data rate increases. It is clear that performance of the rate 1/2 convolutional code is superior to the performance of the rate 3/4 convolutional code. It is possible that designers overestimated the performance of the rate 3/4 convolutional code over a wireless channel. Similar results are presented in [16].

The performance of 16-QAM with a rate 3/4 convolutional code is shown to be inferior to the performance of 64-QAM with a rate 1/2 convolutional code [16]. This thesis models the wireless channel as a Rayleigh fading channel, a subset of the Nakagami channel used in [16]. The combination of studies suggest that the method of combining modulation techniques to coding rates for wireless standards needs to be reconsidered.

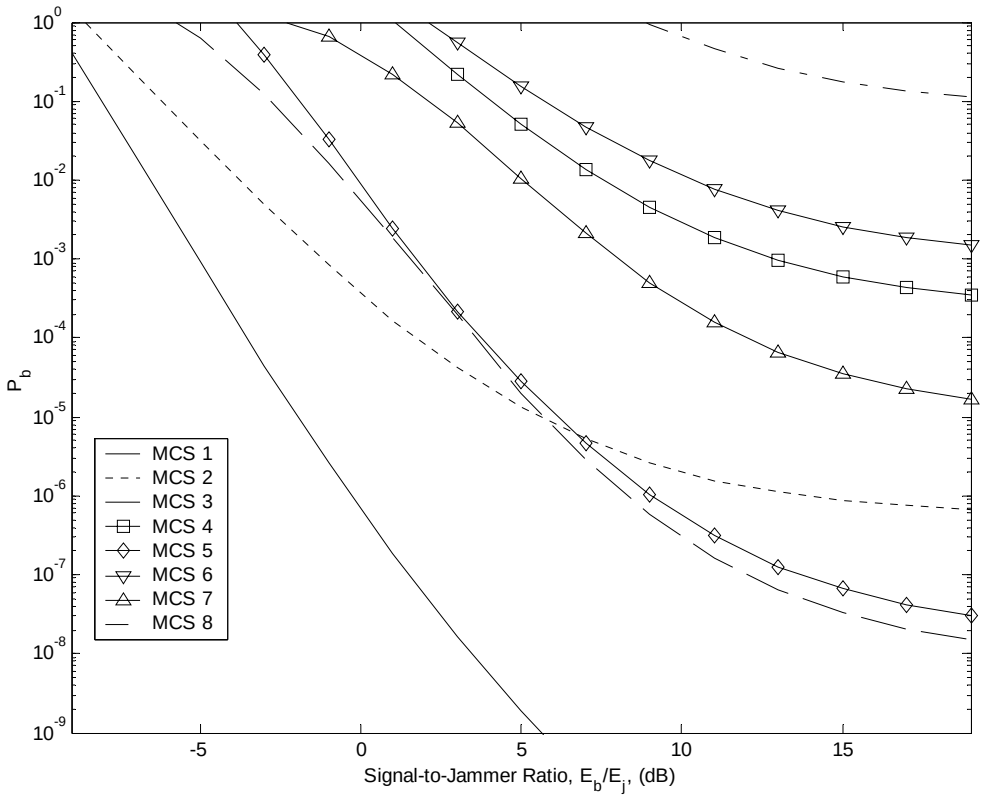

Figure 4.18. Comparison of the Probability of Bit Error for the Modulation and Coding Schemes used in the Packet Data Channel (E_b / N_o =21dB).

Another notable result of the analysis conducted in this thesis is the performance of 8PSK compared to the performance of 16-QAM. The degradation in performance from 8PSK to 16-QAM is minimal. This is especially apparent for rate 1/2 convolutional coding. The lack of significant performance gain by selecting 8PSK over 16-QAM

probably explains why 8PSK is not used in the IEEE 802.11a standard and the proposed cdma2000 standard.

The results of the analysis conducted in this thesis also show that a tone jammer is effective against LAS-CMDA communication. The highest probability of bit error a wireless communication system can tolerate is 10^{-3}. This analysis considers a signal to noise ratio of 21 dB, which is large for cellular systems. The analysis shows that if the received jammer power is equal to the received signal power, LAS-CDMA Packet Data Channel can only communicate using the lowest data rate, 40 kbps per channel. The analysis also shows that the tone jammer is ineffective when the received jammer power is more than 6 dB less the received signal power.

C. FUNDAMENTAL CHANNEL

Unlike the Packet Data Channel, the Fundamental Channel uses a single modulation and convolutional coding rate combination. The Fundamental Channel uses symbol repetition to maintain a constant transmitted bit rate for multiple data rates. The generalized Fundamental Channel parameters are listed in Table 4.4.

Table 4.4. Fundamental Channel Parameters. After Ref [9].

Index	Code Rate	Modulation Type	LS Code Length	Symbol Repetition
FC1	2/3	16 QAM	128	1x
FC2	2/3	16 QAM	128	2x
FC3	2/3	16 QAM	128	4x
FC4	2/3	16 QAM	128	8x

The expression for the probability of symbol error for a 16-QAM, spread spectrum signal given in Equation 4.56 is adjusted for a 128-chip LS spreading code. Equation 4.56 becomes

$$P_{s_I}(\rho)=\left(1-\frac{1}{\sqrt{M}}\right)Q\left(\sqrt{\frac{3E_s}{N_o(M-1)}}+\sqrt{2\frac{E_j}{N_o}}\cos(\theta)\left(\frac{\rho}{128}-\frac{1}{2}\right)\right)$$
$$+\left(1-\frac{1}{\sqrt{M}}\right)Q\left(\sqrt{\frac{3E_s}{N_o(M-1)}}-\sqrt{2\frac{E_j}{N_o}}\cos(\theta)\left(\frac{\rho}{128}-\frac{1}{2}\right)\right) \quad (4.60)$$

For the 128-chip LS spreading codes the probabilities of the valid values of ρ are

$$\Pr(\rho=56)=\frac{7}{32}$$
$$\Pr(\rho=64)=\frac{1}{2}$$
$$\Pr(\rho=72)=\frac{9}{32}$$

The concept of total probability is applied to Equation 4.60. The probability of symbol error of the in-phase 4-PAM component of the 16-QAM signal is

$$P_{s_I}(\rho)=\frac{3}{8}Q\left(\sqrt{\frac{E_s}{N_o 5}}+\sqrt{2\frac{E_j}{N_o}}\cos(\theta)\frac{1}{16}\right)+\frac{3}{8}Q\left(\sqrt{\frac{E_s}{N_o 5}}-\sqrt{2\frac{E_j}{N_o}}\cos(\theta)\frac{1}{16}\right)$$
$$+\frac{3}{4}Q\left(\sqrt{\frac{E_s}{N_o 5}}\right) \quad (4.61)$$

Analogously, the probability of symbol error of the quadrature 4-PAM component of the 16-QAM signal is

$$P_{s_Q}(\rho)=\frac{3}{8}Q\left(\sqrt{\frac{E_s}{N_o 5}}+\sqrt{2\frac{E_j}{N_o}}\sin(\theta)\frac{1}{16}\right)+\frac{3}{8}Q\left(\sqrt{\frac{E_s}{N_o 5}}-\sqrt{2\frac{E_j}{N_o}}\sin(\theta)\frac{1}{16}\right)$$
$$+\frac{3}{4}Q\left(\sqrt{\frac{E_s}{N_o 5}}\right) \quad (4.62)$$

The probability of bit error of the 16-QAM signal spread by a 128-chip LS spreading code in the presence of a tone jammer is found by applying Equation 4.61 and Equation 4.62 to Equation 4.59. Similar to the Packet Data Channel, the assumption is made that Fundamental Channel is transmitted through a Rayleigh fading channel and Equation 4.24 is applied.

The Fundamental Channel uses a rate 2/3 convolutional code to correct errors in the received signal. The first three non-zero values of the information weight structure of the rate 2/3 convolution code used on the Fundamental Channel is listed in Table 4.5. The

first three non-zero values of B_d yield a good approximation of Equation 4.26 and is applied to the probability of bit error.

Table 4.5. Information Weight Structure of the Rate 2/3 Convolution Code Used on the Fundamental Channel. After Ref [15].

d_{free}	B_{dfree}	$B_{dfree+1}$	$B_{dfree+2}$	$B_{dfree+3}$	$B_{dfree+4}$
8	97	0	2863	0	56633

Symbol repetition adds redundancy at the receiver. Some of the received redundant symbols will be more reliable than others. The goal is to make demodulation decisions using the most reliable symbols. The process of symbol repetition can be implemented as time diversity. For purposes of this analysis, it is assumed that the symbols are received independently and that the receiver makes demodulation decision by hard decision, majority vote. Hard decision, majority vote requires the receiver to make individual decisions for each of the received symbols. Then the decisions for all the repeated symbols are combined and the most common symbol is selected as the received symbol.

For symbol repetition with hard decision, majority vote, and the probability that i of the L repeated symbols are received in error is [17]

$$\Pr(error \mid i) = P_s^i \left(1 - P_s\right)^{L-i} \tag{4.63}$$

where P_s is the probability of symbol error. L is even for the symbol repetition patterns used by LAS-CDMA. Since an error occurs when more than half of the repeated symbols are received in error and there is a fifty percent chance of error in the case of a tie, the probability of bit error for a 16-QAM signal when L is even is [17]

$$P_b(L) = \frac{1}{8}\binom{L}{L/2} P_s^{L/2}\left(1-P_s\right)^{L/2} + \frac{1}{4}\sum_{i=\frac{L}{2}+1}^{L}\binom{L}{i} P_s^i\left(1-P_s\right)^{L-i}. \tag{4.64}$$

Figure 4.19 displays the probability of bit error for a 16-QAM, spread spectrum signal with several symbol repetition rates when the signal to noise ratio is 21 dB. The

probability of bit error for a 16-QAM, spread spectrum signal with several symbol repetition rates when the signal to noise ratio is 24 dB is plotted in Figure 4.20.

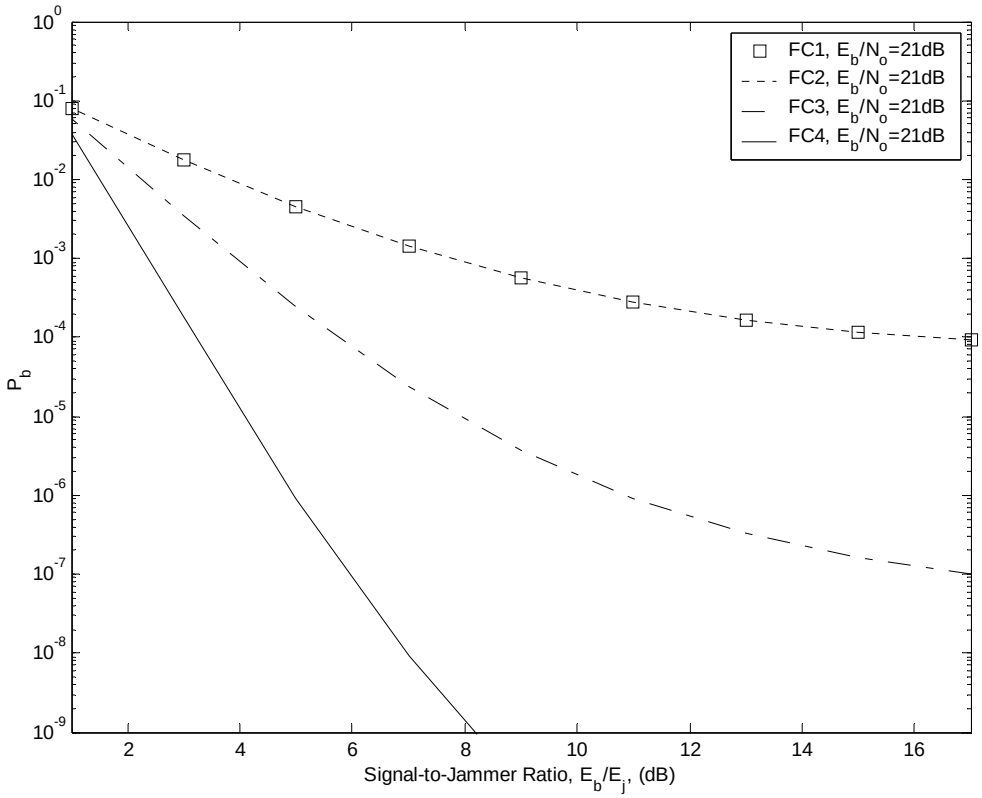

Figure 4.19. Comparison of the Probability of Bit Error for the Symbol Repetition Schemes used in the Fundamental Channel. (E_b / N_o =21dB)

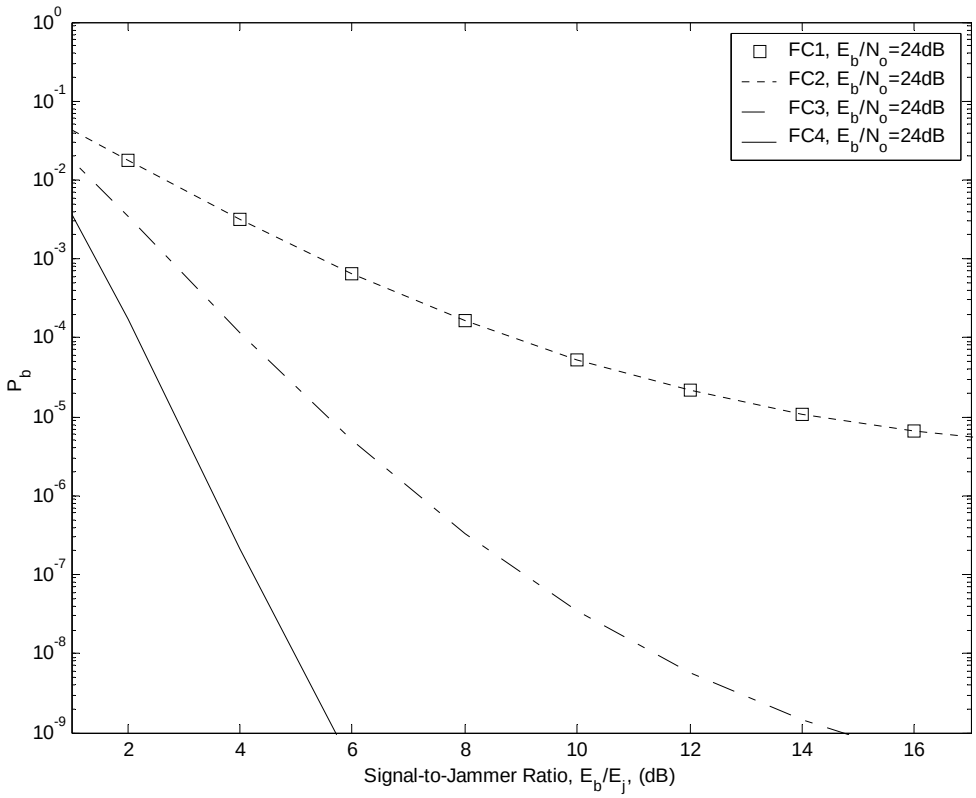

Figure 4.20. Comparison of the Probability of Bit Error for the Symbol Repetition Schemes used in the Fundamental Channel. (E_b / N_o =24dB)

The most notable result of the analysis of the performance of the Fundamental Channel in a Rayleigh fading channel in the presence of a tone jammer is how poor the performance is. For a signal-to-noise ratio of 21dB, the signal must be at least 5dB stronger than the jammer to achieve bit error rates less than 10^{-3}. The signal must be stronger than the jammer to achieve bit error rates less than 10^{-3} when the signal to noise ratio is 24 dB.

It is apparent from this analysis is that for hard decision, detection transmitting the symbol twice does not improve the performance over transmitting the symbol once. Solving Equation 4.64 when L=2, we see that the probability of data symbol error is equal to the probability of channel symbol error. Repeating the symbol twice would improve performance if soft decision detection were used.

Another notable result of this analysis is the decreased benefit of symbol repetition as the probability of channel symbol error increases. The performance gain of symbol repetition decreases more rapidly the more times the symbol is repeated. For a signal to noise ratio of 24 dB and a probability of bit error of 10^{-4}, repeating the symbol four times produces 5 dB of signal-to-jammer gain and repeating the symbol eight times produces 7 dB of signal-to-jammer gain, but for a probability of bit error of 10^{-3} repeating the symbol four times only produces 3 dB of signal-to-jammer gain and repeating the symbol eight times only produces 4 dB of signal-to-jammer gain. For a system designed to operate close to the tolerable limits of the bit error, a tone jammer could be devastating. When transmitting the symbol once or twice close to the limits of the system is unacceptable, decreasing the bit rate and transmitting symbols four times or eight times will only produces modest gains.

THIS PAGE INTENTIONALLY LEFT BLANK

V. CONCLUSION

A. LIMITATIONS

The goal of this thesis was to provide a description of LAS-CDMA, address the security of LAS-CDMA signals, and analyze the effect of a tone jammer on LAS-CDMA in a Rayleigh fading channel. Assumptions are made that limit the application of this thesis. An underlying assumption required to complete this thesis is that the version of the LAS-CDMA standard used as the basis for this thesis is version that will be implemented. There will almost certainly be revisions to the LAS-CDMA standard. The current version makes references to "further study" and "future versions." Alterations to the standard may alter the results of analysis and change conclusions made here.

Another assumption made by this thesis is the statistical model used to describe the fading channel. While the Rayleigh fading channel remains popular, it limits the analysis to communications without a line-of-sight component of the received signal. The Nakagami-m fading channel allows the analysis to be adapted to communications with varying degrees of line-of-sight components included in the received signal. An analysis of the effect of a tone jammer on LAS-CDMA using a Nakagami-m fading channel would allow this thesis to be adapted to a wider range of wireless environments.

B. RESULTS

This thesis finds that LAS-CDMA lacks the security measures taken by other wireless standards to protect transmitted information. Unlike other cellular standards, LAS-CDMA does not mask the spread spectrum information with a long PN sequence . The information transmitted by LAS-CDMA can be intercepted by synchronizing with the Forward Sync Channel and determining the codes used to spread the LAS-CDMA traffic channels. Security of information transmitted by LAS-CDMA needs to be addressed before LAS-CDMA can be implemented as a commercial cellular service.

It is difficult to completely summarize the effect of a tone jammer on LAS-CDMA communications. The results presented in Chapter IV vary depending on the modulation scheme, code rate, and signal-to-noise ratio. In general, the results support the conclusion

that a signal-to-jammer ratio of 0 dB will significantly reduce the performance of LAS-CDMA. A signal-to-jammer ratio of 0 dB would force LAS-CDMA to transmit the Packet Data Channel using QPSK and rate 1/2 convolutional coding to maintain a bit error ratio of 10^{-3} with a signal-to-noise ratio of 21 dB. Without the tone jammer and a signal-to-noise ratio of 21 dB, a bit error ratio of at least 10^{-3} is achieved by transmitting the Fundamental Channel using all of the symbol repetition schemes and transmitting the Packet Data Channel using all of the modulation and code rate combinations except for 16-QAM with rate 3/4 convolutional coding and 64-QAM with rate 3/4 convolutional coding.

The results of the analysis also illustrate the difference between the performance obtained with the rate 1/2 convolutional code and the rate 3/4 convolutional code in a Rayleigh fading channel. For the different modulation and coding schemes used by LAS-CDMA, we expect the performance to degrade as the data rate increases for a given signal-to-noise ratio. From the results of the analysis, we conclude that the performance advantage of the rate 1/2 convolutional code in a Rayleigh fading channel is greater than the performance loss incurred by using higher order modulation schemes. Higher data rates and better performance are provided by higher order modulation and rate 1/2 convolutional coding than lower order modulation and rate 3/4 convolutional coding.

C. RECOMMENDATIONS FOR FURTHER RESEARCH

This thesis leads to topics for future study. One possible topic of future study is improving the security of information transmitted by LAS-CDMA. The feasibility of adapting security techniques to LAS-CDMA could be studied. Another topic for future research is the application of LAS-CDMA spreading codes to other direct sequence spread spectrum systems. The performance of a direct sequence spread spectrum system using Walsh functions could be compared to the performance of the same systems using the LAS-CDMA spreading codes. A more general topic of future study is to prescribe a set of modulation and coding pairs so that as the data rate decreases, the performance in a Rayleigh fading channel increases. This set of modulation and coding pairs could be applied to LAS-CDMA as well as cdma2000 and wireless local area network standards.

LIST OF REFERENCES

[1] Shelia Lam, "First Call for 3.5G," [http://asia.internet.com/asia-news/article/0,,161_678981,00.html], January 2002.

[2] "LinkAir Press Release," [http://www.linkair.com/press-room/press_releases_091301.html], November 2001.

[3] "Chinese Army Bans Cell Phone, Pager Use Among Its Troops," [http://www.navytimes.com/story.php], March 2002.

[4] Z. Anna Entrichel, "Security of Code-Division Multiple Access," MSEE Degree Thesis, Naval Postgraduate School, June 2001.

[5] Cem Sen, "Digital Communications Jamming," MSEE Degree Thesis, Naval Postgraduate School, September 2000.

[6] William C.Y. Lee, *Lee's Essentials of Wireless Communication*, McGraw-Hill, New York, NY, 2001.

[7] Theodore S. Rappaport, *Wireless Communications*, Prentice Hall, Upper Saddle River, NJ, 2002.

[8] Ian Channing, "3G with a Chinese Flavor," Mobile Communications International, August 2001.

[9] China Wireless Telecommunications Standards, *Physical Layer Specification for LAS-2000*, Version 0.3.1, June 2001.

[10] Daoben Li, "A High Spectrum Efficient Multiple Access Code," Fifth Asia-Pacific Conference on Communications, 1999.

[11] Stephen B. Wicker, *Error Control Systems for Digital Communication and Storage*, Prentice Hall, Upper Saddle River, NJ, 1995.

[12] Roger L. Peterson, Rodger E. Ziemer, David E. Borth, *Introduction to Spread Spectrum Communications*, Prentice Hall, Upper Saddle River, NJ, 1995.

[13] Ralph D. Hippenstiel, *Detection Theory; Applications and Digital Signal Processing*, CRC Press, Boca Raton, FL, 2002.

[14] Bernard Sklar, *Digital Communications*, Prentice Hall, Upper Saddle River, NJ, 2001.

[15] R. Clark Robertson, "Class Notes for EC4580, Error Correction Coding," Department of Electrical and Computer Engineering, Naval Postgraduate School, 2002.

[16] Patrick Count, "Performance Analysis of OFDM in Frequency Selective, Slowly Fading Nakagami Channels," MSEE Degree Thesis, Naval Postgraduate School, December 2001.

[17] R. Clark Robertson, "Class Notes for EC4550, Digital Communications," Department of Electrical and Computer Engineering, Naval Postgraduate School, 2002.

INITIAL DISTRIBUTION LIST

1. Defense Technical Information Center
   Ft. Belvoir, Virginia

2. Dudley Knox Library
   Naval Postgraduate School
   Monterey, California

3. National Security Agency, Attn: Bob Eubanks (GRSO/ATD)
   Applied Technologies Division
   Fort George G. Meade, Maryland

4. Cryptologic Research Laboratory, Attn: Nathan Beltz
   Naval Postgraduate School
   Monterey, California

5. Dr. R. Clark Robertson, Department of Electrical and Computer Engineering, Code EC/Rc
   Naval Postgraduate School
   Monterey, California

6. Dr. Tri T. Ha, Department of Electrical and Computer Engineering, Code EC/Ha
   Naval Postgraduate School
   Monterey, California

7. Dr. Jeffrey Knorr, Chairman, Department of Electrical and Computer Engineering.
   Naval Postgraduate School
   Monterey, California

8. Nick Triska
   16 March Pond Ln
   Monroe, Connecticut